CALIBRATION OF A FAR ULTRAVIOLET SPECTROGRAPH AND A STUDY OF VACUUM SPARK BREAKDOWN

By

THOMAS MILTON CARPENTER

Bachelor of Arts

Friends University

Wichita, Kansas

1965

Submitted to the Faculty of the Graduate College
of the Oklahoma State University
in partial fulfillment of the requirements
for the degree of
MASTER OF SCIENCE
May, 1970

NASA CR-102643

CALIBRATION OF A FAR ULTRAVIOLET SPECTROGRAPH AND A STUDY OF VACUUM SPARK BREAKDOWN

By

THOMAS MILTON CARPENTER

Bachelor of Arts

Friends University

Wichita, Kansas

1965

Submitted to the Faculty of the Graduate College
of the Oklahoma State University
in partial fulfillment of the requirements
for the degree of
MASTER OF SCIENCE
May, 1970

NASA CR-102643

Name: Thomas Milton Carpenter Date of Degree: May, 1970

Institution: Oklahoma State University Location: Stillwater, Oklahoma

Title of Study: CALIBRATION OF A FAR ULTRAVIOLET SPECTROGRAPH AND STUDY OF VACUUM SPARK BREAKDOWN

Pages in Study: 113 Candidate for Degree of Master of Science

Major Field: Physics

Scope and Method of Study: A far ultraviolet spectrum from the plasma which is produced by the breakdown of a vacuum spark gap, is analyzed. The spark gap consisted of two, pointed, spectroscopically pure, aluminum electrodes. Data necessary for the analysis is collected and presented. A theory of the use of a spectrum to determine the kinetic electron temperature of a plasma is presented and shown to be impossible with the wavelength range of this spectrograph. The mean kinetic energy of the ions is about 1.1 eV which is at a wavelength of a little over 10,000 Å.

Findings: Several ionic species are definately identified as present in the plasma. A qualitative estimate of the abundance of the ions with from 3 to 7 electrons missing is made.

ADVISOR'S APPROVAL ______________________________

CALIBRATION OF A FAR ULTRAVIOLET

SPECTROGRAPH AND A STUDY OF

VACUUM SPARK BREAKDOWN

Report Approved:

____

Report Adviser

____

____

Dean of the Graduate College

PREFACE

The work presented here was carried out at the suggestion of this student's major advisor, Dr. F. C. Todd. Without his continued and patient direction its completion would not have been possible.

In this report, a spectrum of the far-ultraviolet radiation from the plasma which was formed by the breakdown of an aluminum spark-gap is analyzed. The higher ionization levels are identified and a qualitative determination of the relative abundances is made. A literature survey of spectroscopic methods for determining the plasma temperatures is reported. In addition, the collected data from the spectrum analysis is presented in the appendices.

This student would like to thank Mr. R. D. Payne for the assembly and construction of the spectrograph, which he did as a Masters Degree project. A big vote of thanks also goes to Mr. H. G. Gurney who provided much valuable assistance in the design of the film changer and in obtaining the spectrograms.

A deep appreciation is also expressed for this student's wife, Glenda, whose patience, encouragement and help while carrying out the work was immeasurable. She had the hardest job of all, she prepared the rough draft from hand written copy and she typed the final draft.

Financial support for this work was provided under NASA contract NASr-7.

TABLE OF CONTENTS

LIST OF TABLES

LIST OF FIGURES

CHAPTER I

INTRODUCTION

A study of the impact of a hypervelocity micrometeorite on aluminum was started as an analytical project in 1958 under the direction of Dr. F. C. Todd. Experimentally, it was known that such an impact produced a dense, short lived plasma and that a crater was formed in the aluminum target.

The analytical study at Oklahoma State University resulted in a hydrodynamic model for the plasma. To test the theory and suggest improvements, several experiments were proposed. Three means of producing a spherical aluminum plasma to simulate such an impact were designed. They include a vacuum spark-gap, an exploding wire and the impact of the giant pulse from a laser on an aluminum target.

To obtain data from these plasmas, a spectrograph was designed and constructed by R. D. Payne. The spectrograph has no lens. It employs a grating that is ruled on a concave mirror. The entrance slit, the center of the ruling and the film lie on the Rowland circle in the "so-called" Rowland mounting. The mounting employs grazing incidence (86°) and is entirely enclosed in a chamber which may be evacuated. In its current mode of operation, the range of the spectrograph is from 100 to 1400 angstroms. At 320 angstroms two lines which are separated by 2.4 angstroms are approximately 0.8 centimeters apart. The resolving power is increasingly larger at shorter wavelengths and is decreasingly smaller at longer wavelengths.

The indentification of the ions present, determination of the relative abundances of the ions and the determination of plasma temperatures are among the measurements that may be made with the spectrograph. Temperature determinations and the calculation of relative abundances require intensity measurements as well as the separation of the spectral components.

This report describes the work that is necessary to obtain these measurements. Data on the emission lines in the spectra of Al I through Al VIII was compiled from previously published work. This information may be employed to identify the lines and to predict the relative abundances of the ions. A study of several methods of carrying out the temperature determination was completed and necessary auxiliary data was compiled. To illustrate the use of the compiled data, the spectrum from the breakdown of a vacuum spark-gap was considered and the ions from Al^{+2} to Al^{+6} are identified. As no means of measuring intensity was available, only a qualitative attempt was made to determine the relative abundances. For this particular case, the evidence of the relative intensities show that the ions are not in temperature equilibrium and the intensities indicate the nature and probable reason for the failure to have a temperature equilibrium.

The exploding wire and twin-ruby laser were not operational in time to include the results from these devices in this study. A similar analysis of spectra from each of these will be carried out at a later date.

CHAPTER II

TEMPERATURE MEASUREMENTS

Introduction

The overall objective of the program for which the work in this thesis is one phase, is to determine the characteristics of plasmas by experiment and to correlate these measurements by obtaining analytical expressions for the experimental results. Since the plasmas are probably not in equilibrium at the time that they are formed, it is particularly desirable to simultaneously determine the relative abundance of the ions of different species (singly, doubly, etc. ionized). When these relative abundances are determined, it may be feasible, as was suggested many years ago, to define a temperature for the kinetic energy of the plasma and another temperature for the ions. In contrast, there may be a single temperature for the kinetic energy and the densities of the ionic species may have no temperature based relation to each other. A preliminary analysis of the results on the overall program up to this time, and of the results from this thesis appear to indicate that the latter is the case for the vacuum spark between aluminum electrodes.

Comments on the Following Methods for Temperature Evaluation in This Project

The following survey from the literature presents three methods of determining the temperature by means of spectral studies. These surveys are given to demonstrate that it is impossible to determine the temperature from the information on the spectra that is obtained with this application. Each of the following three methods are applicable under the proper conditions which are discussed in the survey and in the original articles.

The line to continuum method does not require serious consideration for this project. From the preliminary measurements by Willis with the quadrupole mass filter, it is known that the ions and the excited atoms have roughly the same effective temperature with respect to their kinetic energy. This energy corresponds to about 1.1 electron volts. The peak of the continuum radiation from the spark should, according to this measurement, be centered at about 10,000 angstroms. It is certainly not in a range that is recorded by available spectrograph.

The second method from the literature is concerned with relative line intensities. The rough estimate of population intensities from this work and the effective kinetic energy from the quadrupole mass filter show that the relative intensities of the lines in the region that is covered by this equipment cannot be employed. The application requires that the excited ions have a density that is determined by the Boltzman relation. Since the effective, kinetic energy temperature is about 1.1 electron-volts, local thermodynamic equilibrium requires that the ratio of the density of ions and atoms at 1.1 eV to the density of ions that require about 160 eV to ionize is roughly the ratio of 1 to e^{-150}. This would be almost infinitely large; i.e. there would be no Al^{+6} ions. In addition, the "eye ball" estimate of the relative number of ions of each specie cannot satisfy the Boltzman relation. This means that local thermodynamic equilibrium cannot exist.

There is no reason to make any comments on the relative continuum intensities. The continuum intensities are not recorded by the film and data exists for the purpose of comparison.

Relative Line To Continuum Intensities

Looking first to relative line to continuum intensities. Cooper (1960) and Griem (1964) state that this method is restricted to pure gases or when oscillator strengths and continuum emission coefficients are accurately known. Assuming they are known, the development by Cooper is followed.

The total intensity of a given line for path length D in the optically thin case is

(1) $I_t = \frac{h\nu}{4\pi} A(p,q)\ n_{z-1}\ (p)\ D$

where ν = frequency of line

A = coefficient of emission,

and $n_{z-1}(p)$ = number density in the upper state, p.

If the upper state is in equilibrium with electrons and the next higher ionization ground state, $n_{z-1}(p)$ may be stated in terms of Saha's equation.

(2) $n_{z-1}(p) = \frac{g_{z-1}(p)}{2g_z(1)}\ n_e\ n_z(1) \left\{ \frac{2\ \hbar^2}{mkT} \right\}^{3/2} \exp\left\{ \frac{E_{z-1}(\infty) - E_{z-1}(p) - \Delta E_{z-1}(\infty)}{kT} \right\}$

where $g_{z-1}(p)$ = statistical weight of level p

n_e = number density of electrons

$n_z(1)$ = number density of ground state of z ion,

$E_{z-1}(\infty)$ = ionization energy of single z-1 ion

$E_{z-1}(p)$ = energy of level p.

$\Delta E_{z-1}(\infty)$ = lowering of $E_{z-1}(\infty)$ due effect of collection of ions.

Expressing A (p,q) in terms of oscillator strengths, f_{qp}, and statistical weights,

$$(3)\quad A(p,q) = \frac{g(q)}{g(p)} f_{q,p} \frac{8\pi^2 e^2 \nu^2}{mc^3}$$

Then, making the proper substitutions,

$$(4)\quad I_t = D \frac{h\nu}{8\pi} \frac{n_e n_z}{g_z(1)} \left(\frac{2\pi\hbar^2}{mkT}\right)^{3/2} g_{z-1}(q) \frac{8\pi^2 e^2 \nu^2}{mc^3} fqp \exp \frac{E_{z-1}(\infty) - E_{z-1}(p) - \Delta E_z(\infty)}{kT}$$

Continuum radiation which needs to be considered here is two type types: Bremsstrahlung and recombination. Bremsstrahlung is radiation arising from transition of an electron from one free state to another. Physically this is due to collisions between electrons, between ions, or between ions and electrons. In a plasma electron-ion collisions dominate. (Griem, 1964). Recombination radiation is that emitted when an electron goes from a free state to a bound state, i.e., recombines with an ion.

The intensity of Bremsstrahlung and recombination radiation, B+R, for a wavelength interval, $\Delta\lambda = \frac{\lambda^2 \Delta\nu}{c}$, centered at the line being used is

$$(5)\quad I^{B+R}(\Delta\lambda) = \frac{8 e^4 h Z}{3^{3/2} \pi^{1/2} m^2 c^3} \left[g_{ff} \exp\left\{\frac{Z^2 E_H}{kT(g^*+1)^2}\right\} + \sum_{g \geq \left(\frac{Z^2 E_H \lambda}{hc}\right)^{1/2}}^{g^*} \frac{g_{fb}}{g^3} \exp\left\{\frac{Z^2 E_H}{g^2 kT}\right\}\right] \cdot \left[n_e n_z \left(\frac{Z^2 E_H}{kT}\right)^{1/2} \exp\left\{-\frac{hc}{\lambda kT} - \frac{E_{z-1}(\infty)}{kT}\right\} \frac{\Delta\lambda c D}{\lambda^2}\right]$$

where E_H = ionization energy of hydrogen

g^* = is a level above which states are close enough together to be treated as a continuum.

and g_{ff} and g_{fb} = free-free and free-bound Gaunt factors.

Using the relations,

$$E_H = \frac{me^4}{2\hbar^2} \quad ; \quad h\frac{c}{\lambda} = E_{z-1}(p) - E_{z-1}(g)$$

we then get

$$(6)\quad \frac{I_t}{I^{B+R}_{(\Delta\lambda)}} = \frac{3^{3/2}\pi^3}{2\lambda\Delta\lambda}\left(\frac{\hbar^3 c}{m e^4 Z^2}\right)^2 \frac{g_{Z-1}(g)}{g_Z(1)} f_{gp} \frac{\exp\left\{\frac{E_{Z-1}(\infty) - E_{Z-1}(g)}{kT}\right\}}{\left[\frac{g_{ff}}{2}\left(\frac{kT}{E_H}\right)\exp\left\{\frac{E_H}{(g^*+1)^2 kT}\right\} + \sum_{g}^{g^*}\frac{g_{fb}}{g^3}\exp\left\{\frac{E_H}{g^2 kT}\right\}\right]}$$

Several advantages are noted for this formula. It is independent of electron and ion densities and the lowering of the ionization potential cancels. The only remaining factors which are not accurately determined are the oscillator strengths and Gaunt factors. The line intensity, I_t, is that of the entire line profile. Correction is also necessary for the continuum umder the line, which can be made by extrapolation from the line wings.

The main problem in applying this to aluminum would be separation of the continuum intensity due to the different ions present.

Relative Line Intensities

When local thermodynamic equilibrium (LTE) holds, a very reliable method is the comparison of relative intensities for line emission. The method is accurate over the range 75,000 $^{\circ}$K to 5×10^5 $^{\circ}$K. Actually, two methods are used in the comparison of line intensities. One can select lines from the same ionization stages; or lines from successive ionization stages. The greater separation of the energy levels involved in lines from successive ionizations generally make it the more accurate.

The relations for lines from the same ionization will be looked at first. It should be noted that hydrogenic systems were assumed in the derivation of the equations used. The developments here follow those in Griem (1964).

The assumption of LTE leads to the relation for the total intensity, I, for the transition from the level m to n,

(7) $$I_{mn} = \frac{h\omega^3 r_o}{2\pi c} \frac{g_n}{g_m} f_{mn} N_m$$

where r_o - classical radius of the electron

f_{mn} = absorbtion oscillator strength

g_n and g_n = statistal weights of the levels m and n

N_m = density of atoms (n ions) in state m

ω = frequency of line

and the remaining symbols are constant having their usual meaning. The assumption LTE also implies the relation for densities of atoms in the states m and n of the same ionization:

(8) $$\frac{N_n}{N_m} = \frac{g_n}{g_m} \frac{\exp(-E_n/kT)}{\exp(-E_m/kT)}$$

where in addition to the above definations,

E_n = energy of the level, n

and

T = kinetic electron temperature.

Then, taking the ratio of the intensity of two lines,

(9) $$\frac{I'}{I} = \left(\frac{\omega'}{\omega}\right)^3 \frac{g'_n}{g'_m} \frac{g_m}{g_n} \frac{f'_{mn}}{f_{mn}} \frac{N'_m}{N_m}$$

From Eqn. (8) we can substitute for $\frac{N'_m}{N_m}$. Then,

$$\frac{I'}{I} = \left(\frac{\omega'}{\omega}\right)^3 \frac{g'_n}{g'_m} \frac{g_m}{g_n} \frac{f'_{mn}}{f_{mn}} \frac{g'_m}{G_m} \exp\left(\frac{E_m - E'_m}{kT}\right)$$

or

(10) $$\frac{I'}{I} = \left(\frac{\lambda}{\lambda'}\right)^3 \frac{g'_n}{g_n} \frac{f'_{mn}}{f_{mn}} \exp \frac{E_m - E'_m}{kT}$$

or

$$(11)\quad kT = \frac{E_m - E'_m}{\ln \dfrac{I' \lambda'^3 g_n f_{mn}}{I \lambda^3 g'_n f'_{mn}}}$$

The largest uncertainties in this relation are from the determination of oscillator strength, f; the intensities, I; and the relative small separation of the energy levels. The intensity error is purely experimental, depending on choice of lines, and calibration proceedures. Determination of oscillator strengths will be discussed later.

As was mentioned earlier using lines from successive ionizations, which increases the separation of the energy levels involved, will improve the accuracy.

In addition to equations (7) and (8). The following relation for ion densities from successive ionizations is needed.

$$(12)\quad \frac{N_e N_1^z}{N_n^{z-1}} = \frac{2 g_1^z}{g_n^{z-1}} \left(\frac{m k T}{2\pi \hbar^2} \right)^{3/2} \exp\left(- \frac{E_\infty^z - E_n^{z-1}}{kT} \right)$$

where N_e = electron density

N_1 = ground state density

E_∞ = ionization energy

and the other symbols have the same meaning as before. The superscripts Z and Z-1 refer to ionization, Z-1 being the lower.

Taking the intensity of two lines, the one from the higher ionization has that ground state for its lower level because of the occurrence of N_1^z in equation (12).

$$(13)\quad \frac{I^{z}}{I^{z-1}} = \left(\frac{\omega^{z}}{\omega^{z-1}}\right)^{3}\left(\frac{g_1^{z}}{g_m^{z}}\right)\left(\frac{g_m^{z-1}}{g_n^{z-1}}\right)\left(\frac{f_{ml}^{z}}{f_{mn}^{z-1}}\right)\frac{N_m^{z}}{N_m^{z-1}}$$

From (8)

$$(14)\quad N_m^{z} = N_1^{z}\left(\frac{g_m^{z}}{g_1^{z}}\right)\exp\left(\frac{E_1^{z}-E_m^{z}}{kT}\right)$$

Then,

$$(15)\quad \frac{I^{z}}{I^{z-1}} = \left(\frac{\lambda^{z-1}}{\lambda^{z}}\right)\left(\frac{g_m^{z-1}}{g_n^{z-1}}\right)\left(\frac{f_{ml}^{z}}{f_{mn}^{z-1}}\right)\left(\frac{N_1^{z}}{N_m^{z-1}}\right)\exp\left(\frac{E_1^{z}-E_m^{z}}{kT}\right)$$

Substituting from (12) for the ratio $\frac{N_1^{z}}{N_m^{z-1}}$

$$(15)\quad \frac{I^{z}}{I^{z-1}} = \left(\frac{\lambda^{z-1}}{\lambda^{z}}\right)^{3}\left(\frac{g_1^{z}}{g_n^{z-1}}\right)\left(\frac{f_{ml}^{z}}{f_{mn}^{z-1}}\right)\left(\frac{2}{N_e}\right)\left(\frac{mkT}{2\pi\hbar^{2}}\right)^{3/2}\exp\left(-\frac{E_\infty^{z-1}-E_m^{z-1}}{kT}+\frac{E_1^{z}-E_m^{z}}{kT}\right)$$

but, refering all energies to the z-1 ground state;

$$E_1^{z} = E_\infty^{z-1}$$

and

$$E_m^{z} = E_\infty^{z-1} + E_m^{z}$$

Also, correcting for the lower of the ionization potential in a plasma, $-\Delta E_\infty^{z-1}$, we have,

$$(16)\quad \frac{I^{z}}{I^{z-1}} = \left(\frac{\lambda^{z-1}}{\lambda^{z}}\right)^{3}\left(\frac{g_1^{z}}{g_n^{z-1}}\right)\left(\frac{f_{m1}^{z}}{f_{mn}^{z-1}}\right)\left(\frac{2}{N_e}\right)\left(\frac{mkT}{2\pi\hbar^{2}}\right)^{3/2}\exp\left(-\frac{E_m^{z}-E_m^{z-1}+E_\infty^{z-1}-\Delta E_\infty^{z-1}}{kT}\right)$$

The major difficulty in the use of the equation that is derived above is the introduction of the electron density, N_e. This method is valid for large electron densities, i.e., $N_e = 10^{18}$; provided LTE exists. For electron densities even greater than this, the method is very precise. The use of multiplie ionized ions often lead to further inaccuracies. Often the LTE assumption is not as valid, and more difficulty is found in calculating oscillator strengths.

O IV and O V; however, have been used with reasonable accuracy. (Griem, 1964). The configuration of these ions are similar in nature to those of Al III and Al IV, which have been detected in the spark-gap produced plasma.

Relative Continuum Intensities

The comparison of relative line intensities offers a very accurate method of determining temperature using ultraviolet data, providing certain conditions, which have been listed, exist. Relative continuum intensities, however, are independent of most of these restrictions, particularly LTE. Relative continuum intensities then offer what is perhaps the best method of determining plasma temperatures.

Continuum radiation can arise from a multitude of sources. For temperature measurement, in the spectral region under consideration, only three types of radiation need be considered. They are black body, Bremsstrahlung, and recombination.

The problem is usually to determine what type of radiation predominates in a given spectral region. At frequencies for which the absorbtion length is less than the plasma radius, the radiation is black body. When the absorbtion length is large compared to the plasma radius, the radiation is Bremsstrahlung. (Dawson, 1964). The inverse of the absorbtion length is

$$K = \frac{(1.17 \times 10^{-8}) Z N_e^2 \ln \Lambda}{3\nu^2 (kT)^{3/2}} \frac{1}{\left(1 - \frac{\nu_p^2}{\nu^2}\right)^{1/2}}$$

where, kT is in electron volts,

$$\Lambda = \frac{v_T}{\omega_p P_{min}}$$

v_T = thermal velocity of the electrons

$\omega_p = 2\pi\nu_p$ = plasma frequency

P_{min} = minimum impact parameter

= maximum of $\frac{Ze^2}{kT}$ or $\hbar(mekT)^{1/2}$

Assuming that the plasma consists primarily of Al V (Z=4), that $N_e \approx 10^{18}$ and that $kT \approx 30$ eV (values seem reasonable from Bruces work). $\ln\Lambda$ is always of the order 10. Then, at 300 angstroms, the absorbtion length is 8.5 cm, at 1000 angstroms, 0.77 cm, and at 3000 angstroms, 0.085cm. A 2.5 cm. radius is not unreasonable for a laser induced plasma. Assuming this, the cut-off wavelength for black body radiation is 350 angstroms. Comparing this with absorbtion length at 300 angstroms, it is seen that the cut-off is fairly distinct. Above 350 angstroms the radiation can be considered black body and below that wavelength Bremsstrahlung. If N_e were larger, say $N_e \approx 10^{21}$, then at 300 angstroms, the absorbtion length becomes 8.5 x 10^{-6} cm., and the cut-off wavelength for a plasm radius of 2.5 cm. becomes 0.35 angstroms. If the plasma radius was only 1 cm., the cut-off wavelength increases only to 0.87 angstroms.

The intensity, of the radiation at a given frequently from a black body at a specific temperature, is found from the Plank radiation law,

$$I_\nu = \frac{2h\nu^3}{c^2}\left[\exp\left(\frac{h\nu}{kT}\right) - 1\right]^{-1}$$

Temperature determination can then be made by measuring the intensity at two frequencies and taking the ratio, to get

$$\frac{I_{\nu_1}}{I_{\nu_2}} = \left(\frac{\nu_1}{\nu_2}\right)^3 \frac{\exp\left(\frac{h\nu_2}{kT}\right) - 1}{\exp\left(\frac{h\nu_1}{kT}\right) - 1}$$

This must then be solved for T, the temperature.

Consider one other factor, kT. For $N_e \approx 10^{21}$, and the other factors as before, the cut-off wavelengths for black body radiation at kT = 50 eV and kT = 100 ev are respectively 0.81Å and 1.35Å. At $N_e \approx 10^{18}$, these cut-off wavelengths become 81Å and 1350Å.

Thus, on the basis of these rough calculations, only when temperatures are of the order of 100 ev would it no longer be possible to use black body radiation to determine the temperature using the available vacuum ultraviolet spectrograph. Even then, only when the electron densities are low. Such a condition might be expected however, at these high temperatures. In most cases, however, the electron densities would not be this low, and a black body can be assumed, even up to about the 50 ev level.

Should measurements be made that require consideration of Bremsstrahlung and recombination radiation, calculations can be made from the equation presented earlier,

$$I^{B+R}(\Delta\lambda) = \frac{8e^4 h Z}{3^{3/2}\pi^4 m^2 c^3}\left[g_{ff}\exp\left\{\frac{Z^2 E_H}{kT(g^*+1)^2}\right\} + \frac{2Z^2 E_H}{kT}\sum_{g>\left(\frac{Z^2 E_H \lambda}{hc}\right)^{1/2}}^{g^*} \frac{g_{fb}}{g^3}\exp\left(\frac{Z^2 E_H}{g^2 kT}\right)\right] \cdot$$
$$\left[N_e N_Z \left(\frac{Z^2 E_H}{kT}\right)^{1/2} \exp\left\{-\frac{hc}{\lambda kT} - \frac{\Delta E_{Z-1}(\infty)}{kT}\right\}\frac{\Delta\lambda c D}{\lambda^2}\right]$$

In taking the ratio of two intensities the ion and electron densities would cancel as would the correction for the lowering of ionization energy and several constants. The Gaunt factors, g_{ff} and g_{fb}, are slowly varying functions of $\frac{h\nu}{Z^2 E_H}$. Then, if the wavelengths are close enough together, the quantities in the brackets also effectively cancel. This would leave only

$$\frac{I^{B+R}(\Delta\lambda_1)}{I^{B+R}(\Delta\lambda_2)} = \left(\frac{\Delta\lambda_1}{\Delta\lambda_2}\right)\left(\frac{\lambda_1}{\lambda_2}\right)^2 \exp\left[-\frac{hc}{kT}\left(\frac{1}{\lambda_1}-\frac{1}{\lambda_2}\right)\right]$$

There are several advantages in using the method of relative continuum intensities. The independence of LTE has already been pointed out. This would allow checking for LTE, by comparison with results obtained by measuring relative line intensities. Results are also less affected by absorbtion in that as long as the ratios are constant the temperature calculated remains the same.

The method of relative continuum intensities was used by D. W. Gregg and S. J. Thomas to obtain the results published in the March, 1967 issue of Journal of Applied Physics. They studied the temperature a plasma induced by the impact of a laser giant pulse as a function of laser beam intensity. Target materials were beryllium, aluminum and lead.

A prism and grating monochromator were used in series to select the wavelengths used in calculation. The light was then detected by an Amperex 56CVP photomultiplier with the signal being displayed on a Textronix 5(5 oscilloscope. The system was calibrated by replacing the target with a hot tungeston filament. Its black body intensity in the wavelength region being studied was measured and the temperature determined using an optical pyrometer.

The temperature c the plasma was then calculated using the ratio of measured intensities with the Plank law.

Measurements were made at five wavelengths using 50 angstrom wide bands. The centers of the bands were at 10,500Å, 10,100Å, 6100Å, 4000Å. The data is reported in graphic form. For a focused grant pulse intensity of approximately 9 x 10^{10} watts/cm^2, at the three longer wavelengths the temperature of the aluminum plasma was measured at approximately 6 x 10^5 ^oK, or 52 ev.

Comparing the result with that predicted by Bruce(thesis, 1966), there is a good correspondance. Bruce found a maximum temperature of about 43 eV for a spherical plasma of mass 2.17 x 10^{-3} gm. and initial total energy of 2.3 x 10^7 erg. The mass of aluminum displaced by the pulse in Gregg's and Thomas' experiment was at least 1.6 x 10^{-4} gm. Using their formula and figures, the total energy input to the plasma by the pulse was about 2.3 x 10^7 erg.

These results are, then, an indication of order of magnitude of the temperatures to be measured. A smaller wavelength band than Gregg and Thomas used could be obtained using the vacuum ultraviolet spectrograph. The wavelength would be much shorter than they employed; and hence, the hot center could be observed more directly. More exact calculations than presented earlier would be necessary to determine if black body or Bremsstrahlung radiation is being observed at a given wavelength.

CHAPTER III

DATA OBTAINED FROM A SPECTROGRAM

Identification of Observed Lines

The ultraviolet spectrograph was employed to obtain the emitted spectrum from the breakdown of a spark gap between spectroscopically pure aluminum electrodes in a vacuum. A print of the spectrum which was obtained on March 7, 1967 is shown as Figures 1 and 2. The calculated wavelength for each numbered line on the print is tabulated in Table I. The table includes the corresponding wavelength from the published information that is listed in Appendix B, the difference in the calculated and published values, the order of the line and the potential difference for those lines for which the transition has been identified.

Most of the lines for which the wavelength have been calculated are quite distinct, though sometimes faint. The major source of error is focusing which is affected by the large angle of incidence (86^{o}) and other constant angles that are required in calculation. The spectrograph and method of calculation are described in Appendix A.

There are many very faint lines in several regions on the spectrum for which the wavelengths were not calculated. The region from 100 to 200 angstroms, i.e., lines one to eighteen, probably contain

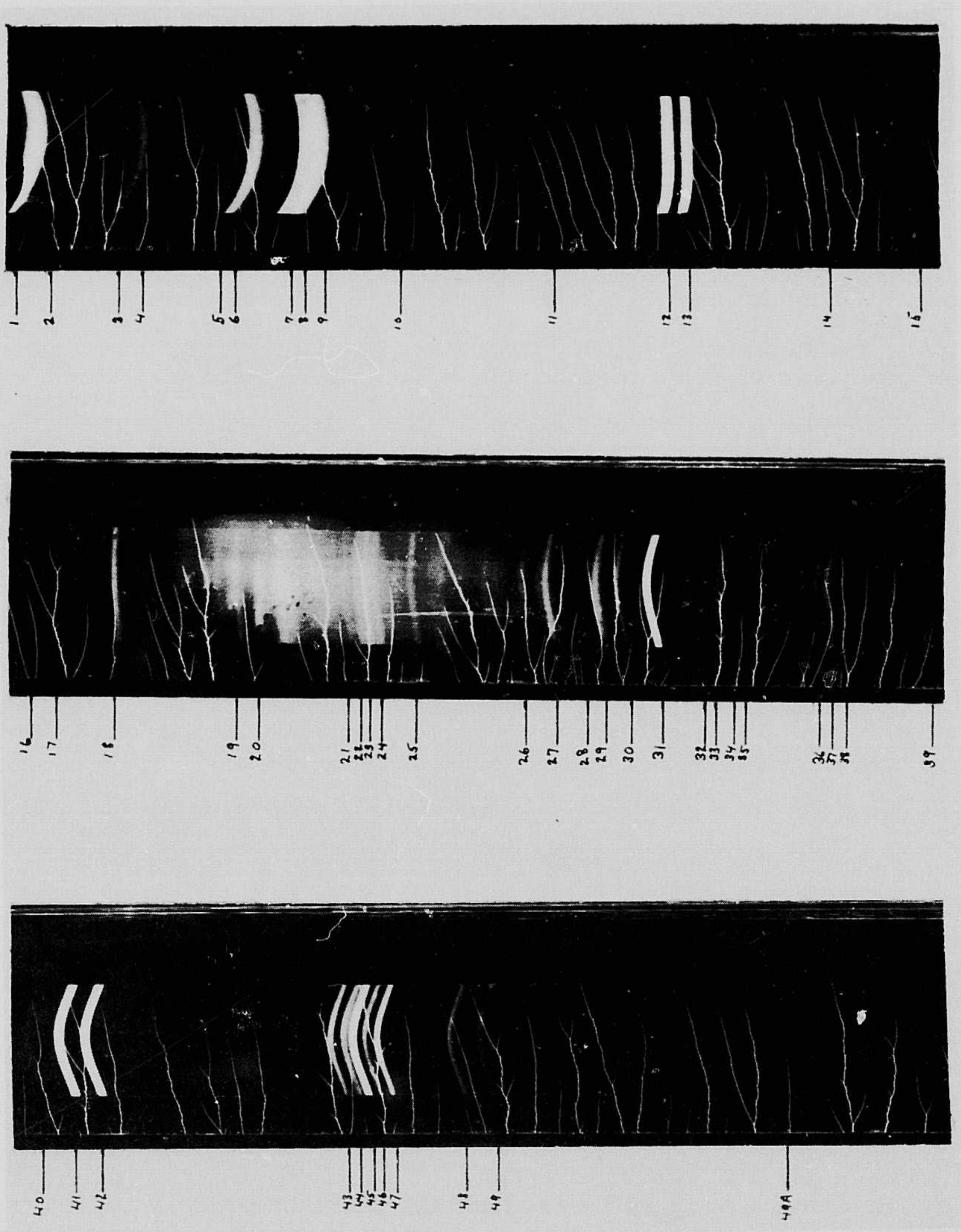

Figure 1. Part I of the Spectrum Analized

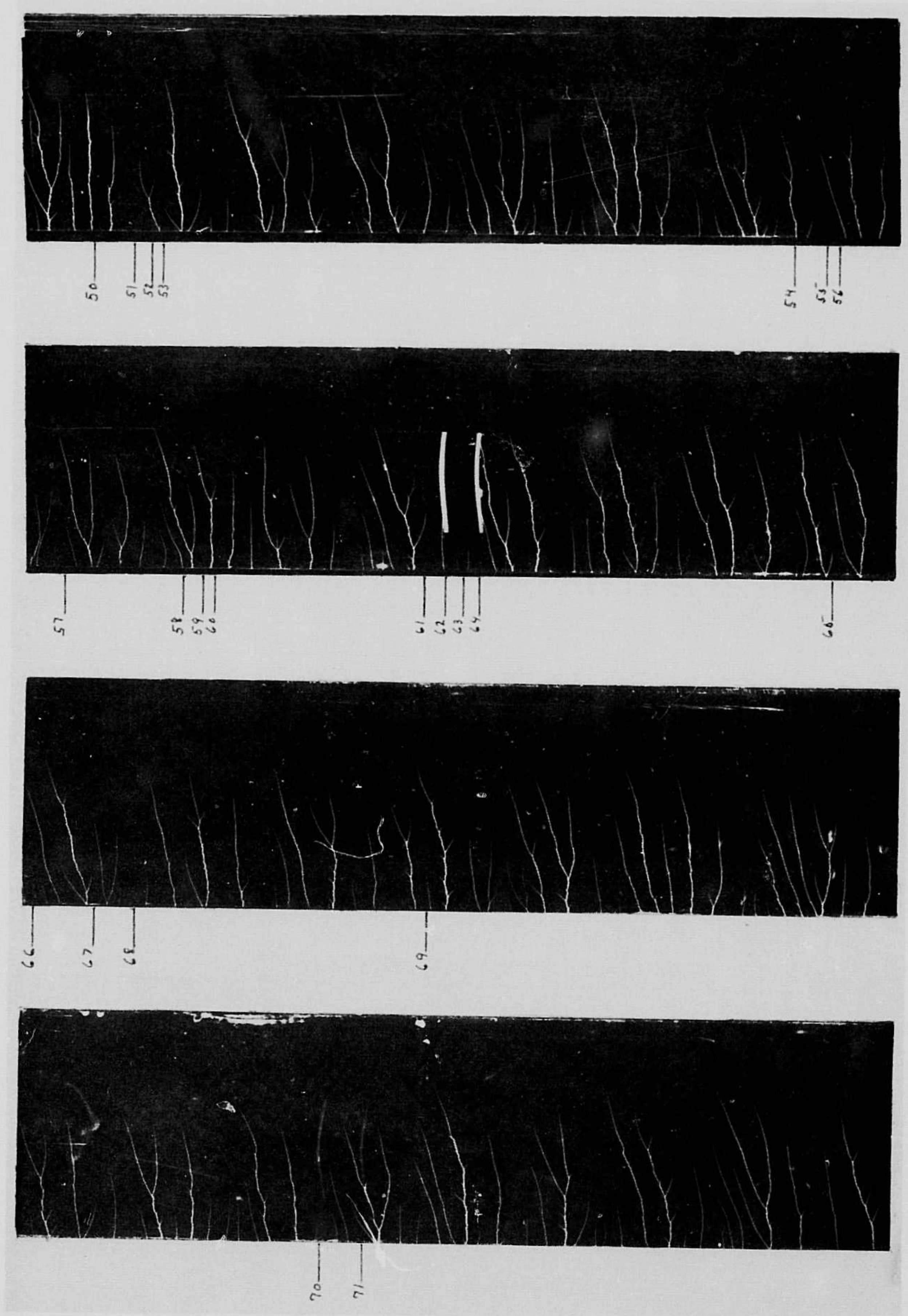

Figure 2. Part II of the Spectrum Analized

TABLE I

LINES OBSERVED IN AN ALUMINUM SPARK SPECTRA

Line No.	Wave Length Calculated	Wave Length Published	Diff.	Order	Ionization
1	110.882	109.514		1	Al VI
		109.843	1.039	1	VI
2	114.014	113.437	0.577	1	VI
3	118.586	116.461		1	IV
		116.921	1.665	1	IV
4	120.534	118.500		1	V
		118.984	2.050	1	V
5	125.614	124.034		1	IV
		124.543	1.071	1	IV
6	127.053	125.525		1	V
		126.065	0.988	1	V
7	131.032	129.729		1	IV
		130.413	0.619	1	V
8	132.218	130.848		1	V
		131.003		1	V
		131.411	0.607	1	V
9	133.742	132.630	1.112	1	V
10	138.822				
11	150.506				
12	160.073		ref.	1	IV
13	161.681	161.686	0.005	1	IV
14	173.027	86.513	0.001	2	VII

TABLE I (Continued)

Line No.	Wave Length Calculated	Published	Diff.	Order	Ionization
15	181.663	91.332	1.001	2	Al VI
16	185.558	92.875	0.192	2	VI
17	187.843	93.955	0.067	2	V
18	192.924	96.150	0.624	2	V
19	204.015	100.919	2.177	2	VI
20	206.216	101.027	4.162	2	VI
21	214.344	107.670		2	VI
		107.945	0.996	2	V
22	215.445	108.057		2	V
		108.112	0.669	2	V
23	216.376	108.385		2	V
		108.402	0.394	2	V
24	217.138	108.707	0.276	2	V
25	220.610				
26	231.193				
27	233.648	116.921	0.194	2	IV
28	237 120	118.500	0.120	2	V
29	238.644	239.030	0.386	1	VII
30	240.760	240.770	0.010	1	VII
31	243.724	243.760	0.036	1	VI
32	247.703	124.034	0.365	2	IV
33	249.058	124.543	0.028	2	IV
34	251.005	125.525	0.045	2	V

TABLE I (Continued)

Line No.	Wave Length Calculated	Published	Diff.	Order	Ionization
35	252.106	126.065	0.024	2	V
36	259.641	129.729	0.183	2	IV
37	260.996	130.413	0.170	2	V
38	262.012	131.006	0.000	2	V
39	272.934				
40	276.067	275.350	0.717	1	VI
41	279.453	278.699	0.754	1	V
42	282.247	281.397	0.850	1	V
43	309.087	307.248	1.839	1	VI
44	310.611	308.560	2.051	1	VI
45	311.542	309.596		1	VI
		309.852	1.690	1	VI
46	312.981	310.908	2.073	1	VI
47	314.336	312.241	2.095	1	VI
48	322.549	160.073	2.403	2	IV
49	326.020	161.686	2.648	2	IV
49A	361.157	356.885	4.272	1	VII
50	390.451				
51	395.870				
52	397.817				
53	399.257				
54	489.935	243.760	2.415	2	VI

TABLE I (Continued)

Line No.	Wave Length Calculated	Wave Length Published	Diff.	Order	Ionization
55	495.015				
56	497.640				
57	513.134				
58	530.575				
59	533.200				
60	535.147				
61	566.812	275.350	16.112	2	Al VI
62	569.860	278.699	12.462	2	V
63	572.993	560.390	12.603	1	III
64	575.448	281.397	12.654	2	V
65	633.445	307.248	18.949	2	VI
66	644.367	312.241	19.885	2	VI
67	655.035				
68	661.639				
69	706.005	695.817	10.188	1	III
70	854.341				
71	862.469				

many second order lines from the first order spectral range of 50 to 100 angstroms. Al VI, Al VII, and Al VIII have many strong lines in this region. In the same region on the spectrogram the focus is not as good as it is on other parts of the spectrogram; hence, the lines are not as well resolved and greater error is possible in determining the wavelength. The 50 to 100 angstrom region also contains several first order lines but these lines should also be present in second order determinations among lines 19 through 53. In the region of lines 19 through 25 some fogging of the film has occurred; hence, measurements on these lines were difficult and are subject to considerable error.

Identification of Ions Present in the Spark

Al III, Al IV, Al V, Al VI and Al VII ions have been identified in the plasma produced by the spark gap breakdown. The identified spectral lines emitted by the plasma are listed by ionic species in Table II . The large number of spectral lines present for Al IV, Al V and Al VI indicate these ions are present in large quantities. Two Al III lines are listed, 560.390 and 695.817 angstroms, but are quite faint. Four Al VII lines have been identified. One of these lines is a second order line and the others are first order. These Al VII lines are stronger than the Al III lines. This evidence and the number of faint lines present in the area where second order Al VII lines should appear indicates that a considerable number of Al VII ions are present.

It should be noted that no attempt has been made to identify possible contaminating elements. The highly possible contaminates,

TABLE II

IDENTIFIED LINES LISTED BY ION SPECIES

Al IV

Wave Length	Wave Number	Term Combination	Order	Rep. Int.	Number
161.686	618483	$2p^6\ ^1S_0 - 3s\ 1\frac{1}{2}\ ^o_1$	1,2	7	13,49
160.073	624715	$2p^6\ ^1S_0 - 3s'\ \frac{1}{2}\ ^o_1$	1,2	8	12,48
129.729	770838	$2p^6\ ^1S_0 - 3d\ 1\frac{1}{2}\ ^o_1$	1,2	6	7,36
124.543	802936	$2p^6\ ^1S_0 - 4s\ 1\frac{1}{2}\ ^o_1$	1,2	3	5,33
124.034	806231	$2p^6\ ^1S_0 - 4s'\ \frac{1}{2}\ ^o_1$	1,2	4	5,32
116.920	855286	$2p^6\ ^1S_0 - 4d\ \frac{1}{2}\ ^o_1$	1,2	2.5	3.27
116.459	858671	$2p^6\ ^1S_0 - 4d\ 1\frac{1}{2}\ ^o_1$	1	3.5	3

Al V

Wave Length	Wave Number	Term Combination	Order	Rep. Int.	Number
281.397	355370	$2p^5\ ^2P^o_{\frac{1}{2}} - 2p^6\ ^2S_{\frac{1}{2}}$	1,2	14	42,64
278.699	358810	$2p^5\ ^2P^o_{1\frac{1}{2}} - 2p^6\ ^2S_{\frac{1}{2}}$	1,2	16	41,62
132.630	753977	$2p^5\ ^2P^o_{\frac{1}{2}} - 3s\ ^4P_{1\frac{1}{2}}$	1	10	9
131.411	760798	$2p^5\ ^2P^o_{\frac{1}{2}} - 3s\ ^2P_{1\frac{1}{2}}$	1	20	8
131.003	763341	$2p^5\ ^2P^o_{\frac{1}{2}} - 3s\ ^2P_{\frac{1}{2}}$	1	20	8

TABLE II (Continued)

Wave Length	Wave Number	Term Combination	Order	Rep. Int.	Number
130.848	764246	$2p^5\ ^2P^o_{1\frac{1}{2}}$ - 3s $^2P_{1\frac{1}{2}}$	1,2	20	8,38
130.413	766795	$2p^5\ ^2P^o_{1\frac{1}{2}}$ - 3s $^2P_{\frac{1}{2}}$	1,2	20	7,37
126.065	793242	$2p^5\ ^2P^o_{\frac{1}{2}}$ - 3s' $^2D_{1\frac{1}{2}}$	1,2	15	6,35
125.525	796654	$2p^5\ ^2P^o_{1\frac{1}{2}}$ - 3s' $^2D_{2\frac{1}{2}}$	1,2	15	6,34
118.984	840449	$2p^5\ ^2P^o_{\frac{1}{2}}$ - 3s" $^2S_{\frac{1}{2}}$	1	6	4
118.500	843882	$2p^5\ ^2P^o_{1\frac{1}{2}}$ - 3s" $^2S_{\frac{1}{2}}$	1,2	10	4,28
108.707	919904	$2p^5\ ^2P^o_{1\frac{1}{2}}$ - 3d $^4D_{2\frac{1}{2}}$	2	6	24
108.462	921982	$2p^5\ ^2P^o_{\frac{1}{2}}$ - 3d $^2D_{1\frac{1}{2}}$	2	10	23
108.385	922637	$2p^5\ ^2P^o_{1\frac{1}{2}}$ - 3d $^4P_{2\frac{1}{2}}$	2	10	23
108.112	924967	$2p^5\ ^2P^o_{\frac{1}{2}}$ - 3d $^2P_{1\frac{1}{2}}$	2	12	22
108.057	925438	$2p^5\ ^2P^o_{1\frac{1}{2}}$ - 3d $^2D_{1\frac{1}{2}}$	2	12	22
107.945	926398	$2p^5\ ^2P^o_{1\frac{1}{2}}$ - 3d $^2D_{2\frac{1}{2}}$	2	20	21
96.150	1040040	$2p^5\ ^2P^o_{\frac{1}{2}}$ - 4s' $^2D_{1\frac{1}{2}}$	2	1	18
93.955	1064340	$2p^5\ ^2P^o_{\frac{1}{2}}$ - 4d $^2P_{1\frac{1}{2}}$	2	6	17

Al VI

Wave Length	Wave Number	Term Combination	Order	Rep. Int.	Number
312.241	320365	$2p^4\ ^3P_1$ - $2p^5\ ^3P^o_2$	1,2	3	47,66
310.908	321639	$2p^4\ ^3P_0$ - $2p^5\ ^3P^o_1$	1	3	46

TABLE II (Continued)

Wave Length	Wave Number	Term Combination	Order	Rep. Int.	Number
309.852	322735	$2p^4\ {}^3P_1 - 2p^5\ {}^3P^o_1$	1	2	45
309.596	323002	$2p^4\ {}^3P_2 - 2p^5\ {}^3P^o_2$	1	4	45
308.560	324086	$2p^4\ {}^3P_1 - 2p^5\ {}^3P^o_0$	1	3	44
307.248	325470	$2p^4\ {}^3P_2 - 2p^5\ {}^3P^o_1$	1,2	3	43,65
275.350	363174	$2p^4\ {}^1S_0 - 2p^5\ {}^1P^o_1$	1,2	3	40,61
243.760	410240	$2p^4\ {}^1D_2 - 2p^5\ {}^1P^o_1$	1,2	6	31,54
113.437	881547	$2p^5\ {}^3P^o_2 - 3s''\ {}^3P_2$	1	3	2
109.843	910391	$2p^4\ {}^3P_1 - 3s\ {}^3S^o_1$	1	12	1
109.514	913125	$2p^4\ {}^3P_2 - 3s\ {}^3S^o_1$	1	20	1
107.620	929195	$2p^4\ {}^1D_2 - 3s'\ {}^1D^o_2$	2	14	21
101.027	989834	$2p^4\ {}^3P_0 - 3s''\ {}^3P^o_1$	2	3	20
100.919	990894	$2p^4\ {}^3P_1 - 3s''\ {}^2P^o_{0,1}$	2	4	19
92.875	1076720	$2p^4\ {}^3P_0 - 3d\ {}^3D^o_1$	2	10	16
91.332	1094910	$2p^4\ {}^1D_2 - 3d'\ {}^1P^o_1$	2	10	15

Al VII

Wave Length	Wave Number	Term Combination	Order	Rep. Int.	Number
356.885	280202.3	$2p^3\ {}^4S_{1\frac{1}{2}} - 2p^4\ {}^4P_{2\frac{1}{2}}$	1	5	49A
240.770	415334.1	$2p^3\ {}^2D^o_{2\frac{1}{2}} - 2p^4\ {}^2P_{1\frac{1}{2}}$	1	4	29
239.030	418357.5	$2p^3\ {}^2D^o_{1\frac{1}{2}} - 2p^4\ {}^2P_{\frac{1}{2}}$	1	2	30

TABLE II (Continued)

Wave Length	Wave Number	Term Combination	Order	Rep. Int.	Number
86.887	115092.0	$2p^3\ {}^2D^o_{1\frac{1}{2}}$ - $3s\ {}^4P_{2\frac{1}{2}}$	2	18	14

Al III

Wave Length	Wave Number	Term Combination	Order	Rep. Int.	Number
695.817	143716.0	$3s\ {}^2S_{\frac{1}{2}}$ - $4p\ {}^2P^o_{1\frac{1}{2}}$	1	5	69
560.390	178447.2	$3s\ {}^2S_{\frac{1}{2}}$ - $5p\ {}^2P^o_{\frac{1}{2},1\frac{1}{2}}$	1	7	63

oxygen and nitrogen, do have several strong lines in the range of the spectrogram.

The transition involved for each line listed in Table II for Al IV, V and VI is shown on the corresponding energy level diagrams in Figures 3, 4 and 5. For each energy level is listed the term designation, the outer electron configuration, the excitation energy (relative to the ground state for that ion) in wave number, and the total angular momentum quantum number J. Also listed on the figure is the ionization potential of that ion in wave number. As can be readily observed on the figure most of the lines involve transitions to the ground state.

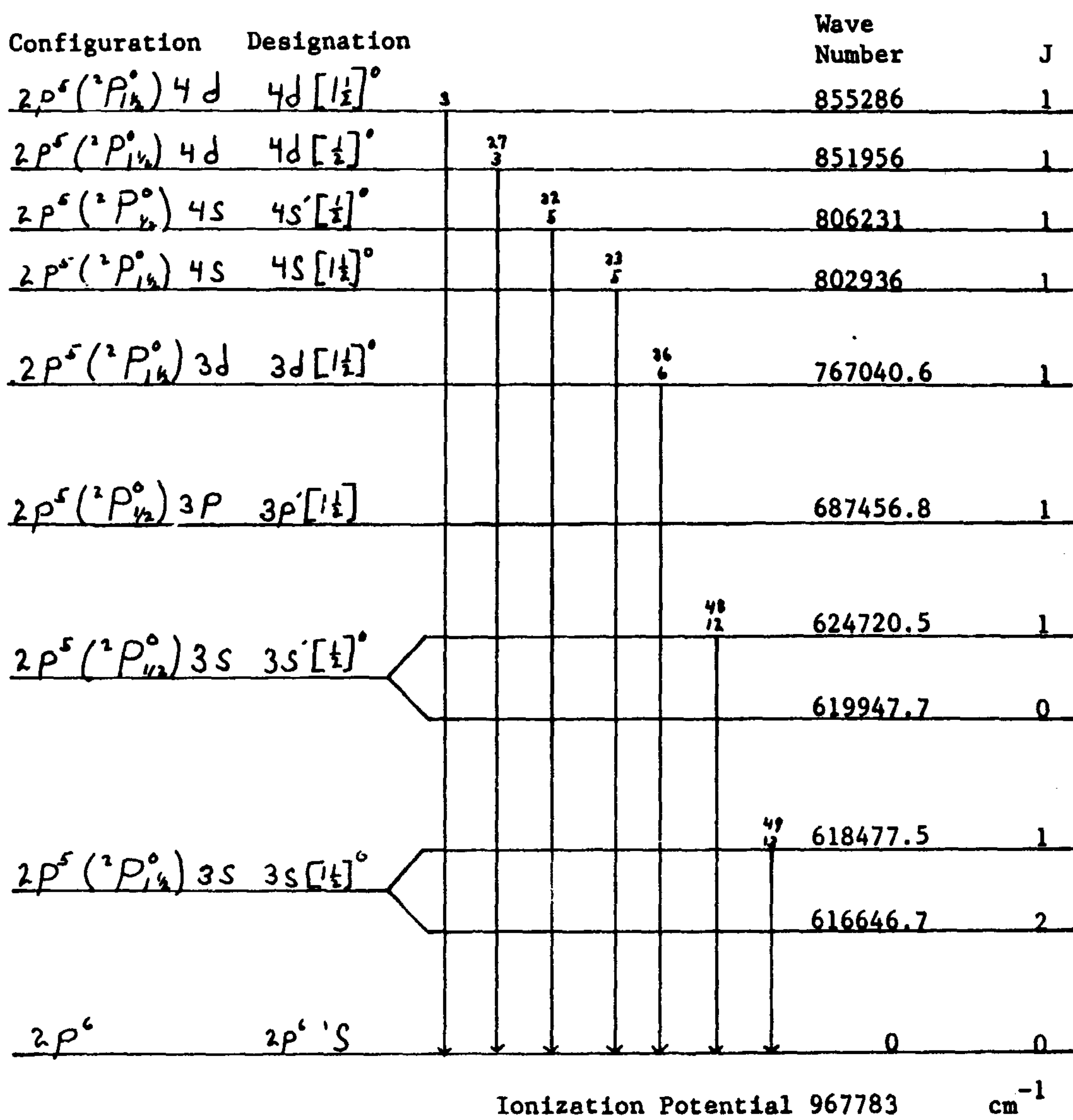

Figure 3. Observed Al IV Energy Level Transitions

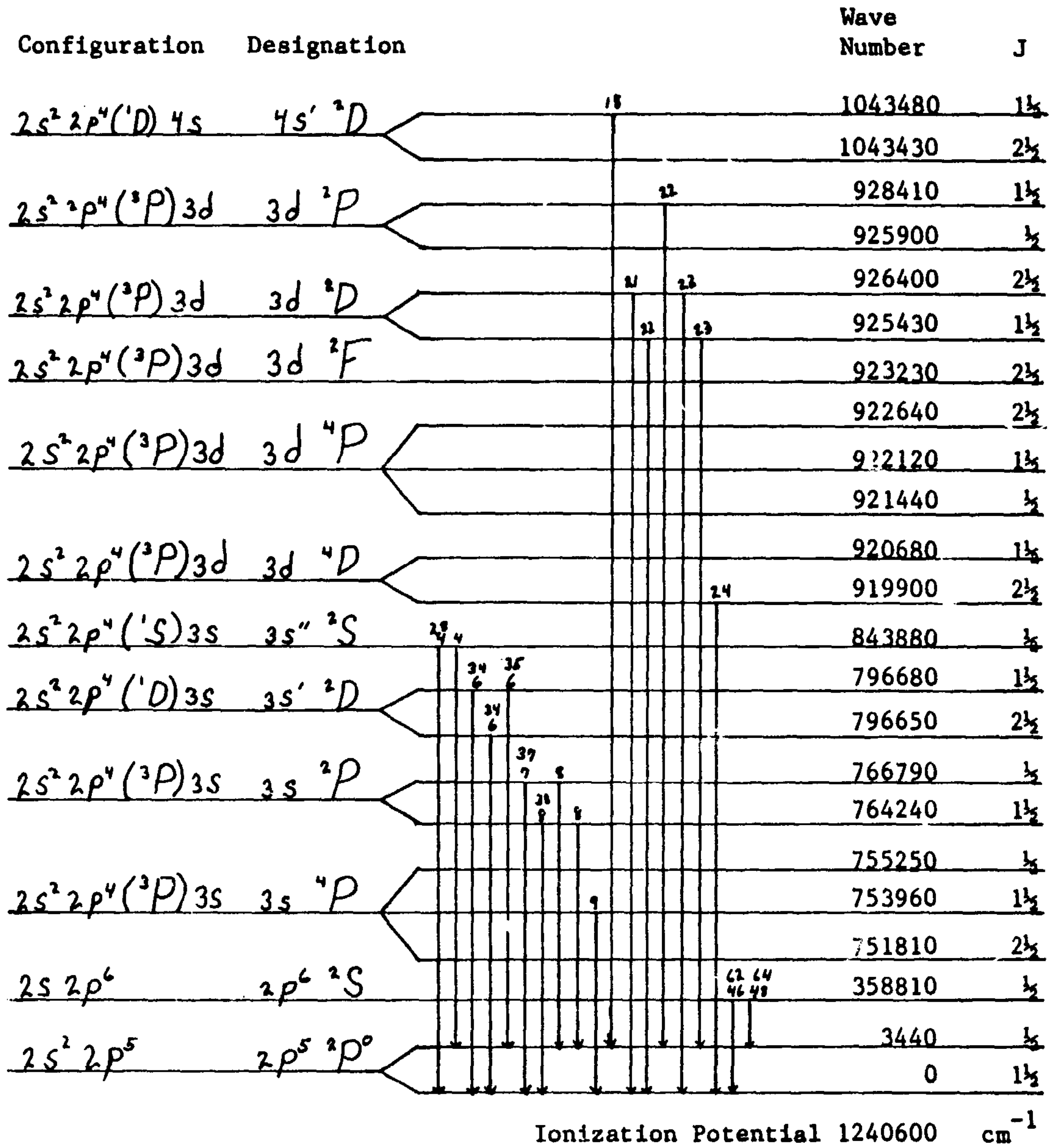

Figure 4. Observed Al V Energy Level Transitions

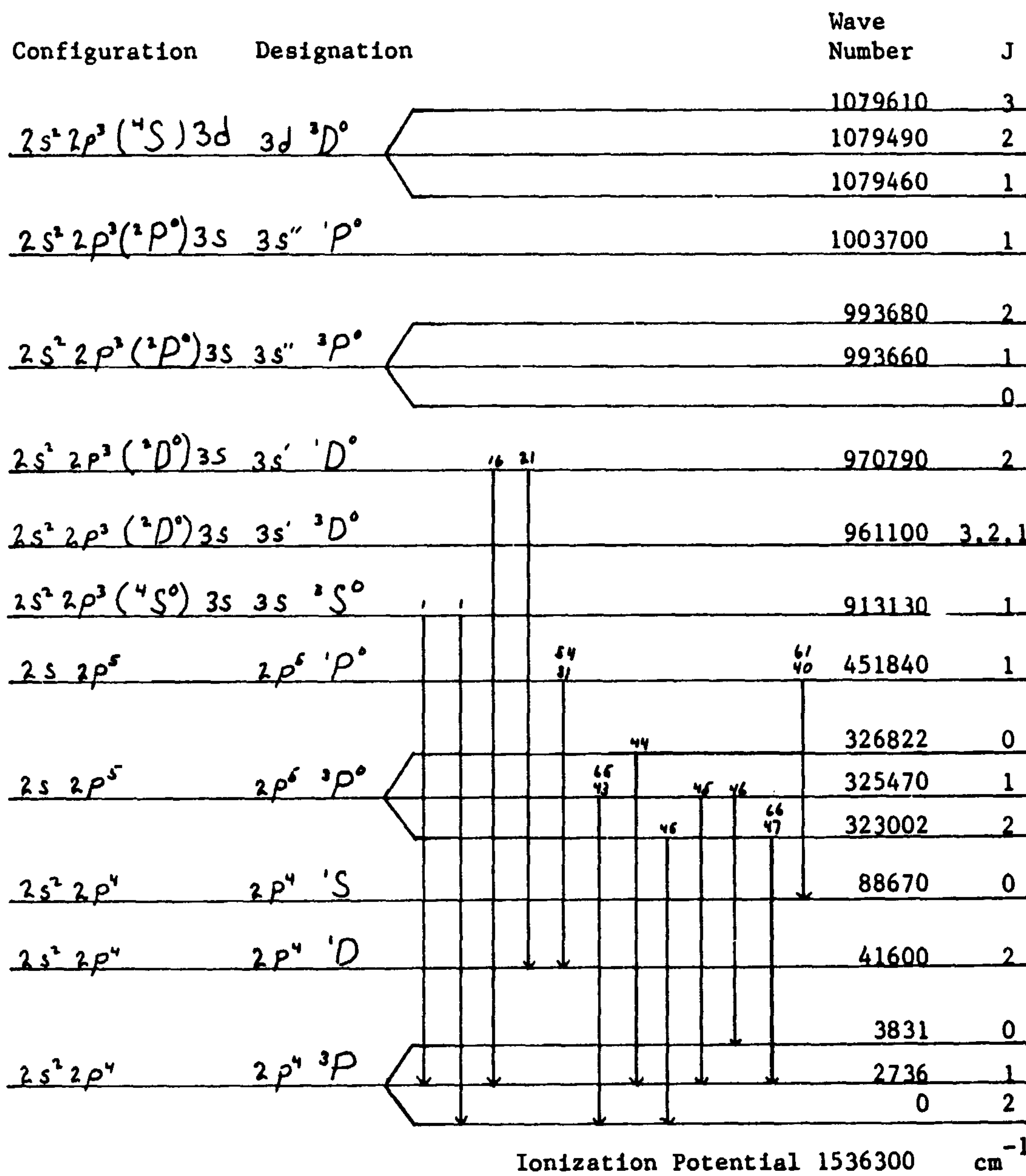

Figure 5. Observed Al VI Energy Level Transitions

CHAPTER IV

ANALYSIS OF RESULTS

The data that were obtained during the experimental program for this thesis are presented in an earlier section of this report. This data consists of a list that gives the lines that are observed in one of the many spectra that were photographed. The table also identifies the transition that is responsible for each line and reports the relative intensity of the lines. Prior to a presentation of an analysis of the preceeding data, it is desirable to give a short review of the characteristics of the source that is employed to produce a spectrum. This is followed by a review of the characteristics and spectral range of the ultraviolet spectrograph that was employed. This description also identifies the short wavelength limit of each spectral class; that is, Al I, Al II, Al III, etc. This is followed by an "eye-ball" analysis of the data in order to obtain a little information on the relative abundance of the different ions.

Source of the Spectral Lines

The source for the spectral lines is a vacuum spark gap with spectroscopically pure aluminum electrodes. The energy for the spark is supplied by a 1.0 microfarad condenser that is charged to 12,500 volts. The conducting channel between the electrodes starts as a very thin thread of a dense aluminum plasma and expands very rapidly in the radial directions. This statement is in rough accordance with the existing concepts of breakdown (Meek and Craggs, 1953). More important for the interpretation of the results, the studies by Brown for his EdD thesis (Brown, 1968) give very strong confirmation of the initial, thin thread and of the subsequent, rapid, radial expansion.

Spectrograph for the Ultraviolet

The spectrograph for the far ultraviolet covers the spectral range from 100 Å to 1400 Å. The grating has 30,000 lines per inch and is used at almost grazing incidence. The angle of incidence is 86° which is measured between the normal to the grating and the angle of incidence of the light. At this angle of incidence, the aberrations from the grating are extremely bad and a great deal of very delicate adjustments are required to minimize them and to obtain a good spectrogram. Each adjustment, which is made one at a time and checked with a photograph of the spectrum, is followed by another adjustment with another check with a photograph. The final adjustments are attained after months of work and this alignment of the spectrograph is the real contribution of this thesis.

Since the spectrograph employs the grating at grazing incidence, the resolution varies with the wavelength. The resolution is largest at short wavelengths and decreases as the wavelength increases. There is another very important consequence of grazing incidence which is coupled with the fact that the grating is ruled with no blaze. The term, no blaze or zero blaze, is the optical designation when the light is reflected from the undisturbed original surface that is between the rulings; i.e., the reflecting strips are the unchanged, original surface of the concave mirror. The reflecting surfaces are between the very light scratches that are made by the ruling engine.

The intensity of the lines in the spectrum is always the greatest when the line is deviated by the least amount from the angle of reflection. The angle of incidence is 86° and the angle of reflection will be 86°. The spectral lines must make smaller angles, less than 86°, with the normal to the grating. This means that the reflected lines are much more intense in the short wavelength range than in the long wavelength range. In fact, only the very strongest lines--from the amount of emitted light from the spark--are even observed at wavelengths that are longer than 1000 Å. If intensities are to be compared, the line for comparison should be bracketed by known reference lines for the most accurate comparison. Although it may be very troublesome to interpret, lines in different positions on the film may be compared directly by calculating the correction factor for the intensity.

In the preceeding tables, the spectral lines are tabulated under the designations of the spectra for Al I, Al II, etc. The short wavelength limit of Al I is given as the ionization potential of the aluminum atom. The designation, spectrum of Al I, is the spectrum of the excited aluminum atom, Al*. In a similar manner, the spectrum of Al II extends from the ionization potential of Al^+ down into and overlapping the spectrum of Al I. The ionization potentials for aluminum atoms and for the first seven ions are given in Table III with the corresponding ionization potentials and with the short wavelength limits.

TABLE III

SHORT WAVELENGTH LIMIT BY SPECTRAL DESIGNATION AND BY THE DEGREE OF IONIZATION

Spectral Designation	Ionization Potential eV	Short Wavelength Limit Å	Ion
Al I	5.984	2071.9	Al^*
Al II	18.823	658.65	Al^+
Al III	28.44	435.93	Al^{+2}
Al IV	119.96	103.35	Al^{+3}
Al V	153.77	80.63	Al^{+4}
Al VI	190.42	65.11	Al^{+5}
Al VII	241.93	51.25	Al^{+6}
Al VIII	285.13	43.48	Al^{+7}

Comparison of Detected Ions

The results in Chapter III indicate the presence of Al III, Al IV, Al V, Al VI, and Al VII ions in the spark gap plasma. Any evaluation of the relative abundances of these ions, even qualitative, is very difficult. The comparison of line intensities for this purpose is complicated by the effect of the blaze of the diffracting grating. This grating has a zero blaze so that most of the intensity falls near the central image; i.e., in the short wavelength region. Lines of equal intensity would appear to diminish in intensity as the wavelength increases.

The effect of the blaze accounts for the weak intensity of the Al III lines, although the current theoretical work by Perry and experimental evidence by Willis from a mass filter indicate that these ions are present in large quantities. All six Al III lines which may be detected on the spectrograph are in the upper end of its wavelength range. Only the two shortest wavelengths of these six are observed and they are faint lines on the spectrogram.

Most Al IV, Al V, Al VI and Al VII lines are of shorter wavelengths and are nearer to the central image. They may be expected to be and they are more intense on the film. The effect of the blaze may be minimized and a very rough, qualitative estimate of relative abundances may be obtained by comparing lines that are close together on the film.

The comparison is made using the relative density of lines which is visually estimated on a 0-10 scale. Film density, however, is proportional to the natural logarithm of the exposure. This means that the exposure may be related to the relative abundances.

The ratio of two densities is

$$\frac{D_1}{D_2} = \frac{\ln E_1}{\ln E_2}$$

Since the relative abundances are desired, $\ln E_2$ may be arbitarily set equal to 1 in order to obtain this relation

$$\ln E_1 = \frac{D_1}{D_2} ,$$

or

$$E_1 = \exp\left(\frac{D_1}{D_2}\right).$$

Dividing by $E_2 = e$

$$\frac{E_1}{E_2} = \exp\left(\frac{D_1}{D_2} - 1\right)$$

This relation gives the ratio of abundance when lines from different spectra, Al I, etc, are compared. The lines have equal strengths when the abundances are equal. Lines of unequal intensity may be compared by setting the exposure, E, equal to the product of the reported intensity, w, and a value, A, which is proportional to the abundance as indicated in the following relation.

$$\frac{E_1}{E_2} = \frac{w_1}{w_2}\frac{A_1}{A_2} = \exp\left(\frac{D_1}{D_2} - 1\right)$$

Al IV and Al V are compared by employing lines 3 and 4 of Figure 1. Line 3 cons[illegible] of two, unresolved, first order Al IV lines. Line 4 consists o[illegible] o, unresolved, first order Al V lines. The two Al IV lines have published intensities of 7 and 5 while the two Al V lines both have published intensities of 6. All the intensities are from a 1934 article by Jonas Soderqvist. The densities of lines 3 and 4 are visually estimated as 3 and 2 respectively. The resulting ratio of abundances, $\frac{\text{Al IV}}{\text{Al V}}$, is 1.64.

Al V and Al VI are compared by employing lines 40 and 41. Line 41 is a first order, Al V line of published intensity 14. Line 40 is a first order, Al VI line of published intensity 6. Both intensities are from the 1934 article by Soderqvist. Visual estimates of the densities are 1.5 and 7 for lines 40 and 41 respectively. The resulting ratio of abundances, $\frac{\text{Al V}}{\text{Al VI}}$, is 16.5.

Al VI and Al VII are compared by employing lines 29, or 30, and 31. Line 31 is a first order Al VI line and lines 29 and 30 are first order Al VII lines. The published intensities for 29, 30, and 31 are 4, 2, and 12, respectively from the 1934 article by Soderqvist. The estimated densities are 3, 2, and 6 for lines 29, 30, and 31. Using lines 30 and 31 the ratio of abundances, $\frac{\text{Al VI}}{\text{Al VII}}$, is 1.21.

The abundances can be stated in terms of fractions of the abundance of Al IV as follows:

$$Al^{+3} = \text{Al IV} = 1.00 \text{ Al IV}$$
$$Al^{+4} = \text{Al V} = 0.61 \text{ Al IV}$$
$$Al^{+5} = \text{Al VI} = 0.037 \text{ Al IV}$$
$$Al^{+6} = \text{Al VII} = 0.030 \text{ Al IV}$$

While the qualitative nature of the above results must be emphasized and the particular values cannot be considered reliable a valuable rough estimate of the integrated, average abundances of the higher order ions is obtained. It is immediately apparent that these high energy ions are not in equilibrium. This is immediately evident from the energy that is required to obtain Al^{+3}, Al^{+4}, etc. The significance of these results is discussed in the following section.

CHAPTER V

CONCLUSIONS

The results from the rough, "eye-ball" evaluation of the spectra indicates the possibilities that may be inherent in an accurate interpretation of the data. The significance of the results are best illustrated by a short description of our knowledge of the vacuum breakdown between the spectroscopically pure aluminum electrodes. This information is acquired as an additional dividend that reslts from employing the vacuum spark to calibrate (1) the pulsed photomultiplier, (2) the quadrupole mass filter and (3) the far ultraviolet spectrograph. These are the three plasma measuring techniques that have been developed on this project for the study of dense plasmas. The calibration and use of item 3 is the subject of this thesis.

It is postulated in the literature (Meeks and Cragg, 1953) that the spark current is initially carried by a thin column of aluminum plasma. The results that were obtained by Brown with the pulsed photomultiplier appear to confirm the analytical study by (Bruce, 1966) on an expanding plasma. Provided this confirmation exists, the plasma thread expands very rapidly and is relative opaque to the radiation from the ions Al^{+3}, Al^{+4}, Al^{+5} and Al^{+6}.

Measurements with the quadrupole mass filter appear to show that the kinetic energy of the exicted aluminum atom, Al* , and of the ions Al^{+1}, Al^{+2} and Al^{+3} is the same. From this result, it appears that the atoms, excited atoms and ions are in kinetic energy equilibrium. The equilibrium temperature is estimated to be 12,200 ^{o}K, or roughly 1.1 eV in different units.

From the results on the relative abundance of ions that are estimated in this thesis, it is believed that the spectra from Al IV, Al V, Al VI and Al VII indicate a relative abundance of 1.0, 0.6, 0.037 and 0.030. Since the ionization potentials for these four ions are 119.96, 153.77, 190.42. 241.93, there is no single temperature for insertion in a Boltzmann relation that will give these relative abundances. This should probably be anticipated, but is is aftersight rather than foresight. During the entire time that voltage is applied to the gap, one could speak of a mean free path for the electrons. The preceeding data appears to indicate that the mean free path in the field is sufficiently long so the electrons acquire an average energy of between 160 and 130 eV, in the field between the ionization-collisions. This interpretation presents a new, reasonably sound approach to the study of the attainment of equilibrium. An extension and more accurate evaluation of the spectra with densitometers should prove extremely valuable.

SELECTED BIBLIOGRAPHY

(1) Allen, C. W. Astrophysical Quantities. London: the Athlone Press, 1955.

(2) Bowen, I. S., and S. B. Ingram. "Wave-length Standards in the Extreme Ultraviolet Spectra of Carbon, Nitrogen, Oxygen, and Aluminum." Physical Review, Vol. 28. (September, 1926), p. 444.

(3) Boyce, J. C., and H. A. Robinson. "Wave-length Identification Lists For the Extreme Ultraviolet." Journal of the Optical Society of America, Vol. 26, No. 4. (April, 1936). p. 133.

(4) Brown, V. D. and F. C. Todd. "Use of a Pulsed Photomultiplier to Measure the Light Intensity versus Time for a Spark Discharge Between Aluminum Electrodes." (unpublished Ed.D. dissertation, Oklahoma State University, 1968).

(5) Bruce, R. E. "A Model and Calculations For the Properties of an Exploding Plasma Sphere." (Ph.D. Thesis, Oklahoma State University, 1966).

(6) Chandrasekhar, S. An Introduction to the Study of Stellar Structure. New York: Dover, (1957).

(7) Cooper, J. "Plasma Spectroscopy." Reports on Progress in Physics, London. Vol. XXIX (1966), pt. I, pp. 35.

(8) Dawson, J. M. "On the Production of Plasma by Giant Pulse Lasers." The Physics of Fluids, Vol. 7, No. 7, (July, 1964) p. 981.

(9) Ekefors, E. "Das Spektrum Von Al in Extremen Ultraviolet." Zeitschrift fur Physik, Band 51, (1928), p. 471.

(10) Erikson, K. B. S., and H. B. S. Isberg. "The Spectrum of Atomic Aluminum, Al I." Arkiv For Fysik, Band 23, nr 47, (1963), p. 527.

(11) Ferner, E. "Die Spektren von Hochionisiertem Aluminum, Silicium, und Schwefel." Arkiv for Matematik, Astronomi, und Fysik, Band 36A, No. 1, (1949), p. 1.

(12) Gregg, D. W., and S. J. Thomas. "Plasma Temperatures Generated by Focused Laser Giant Pulses." Journal of Applied Physics, Vol. 38, No. 4, (March 15, 1967), pp. 1729-1731.

(13) Griem, H. R. Plasma Spectroscopy, New York: McGraw-Hill, (1964).

(14) Griem, H. R. Temperature; Its Measurement and Control in Science and Industry, Vol. 3, pt. 1, Ed. C. M. Herzfeld. New York: Reinhold, (1962), p. 615.

(15) Hardage, Bob Adrian. "Hypervelocity Impact with Flow and Shock Penetration Through Fluid, Plastic and Elastic Zones." (Unpublished Ph.D. dissertation, Oklahoma State University, 1967).

(16) Hill, W. E. Temperature: Its Measurement and Control in Science and Industry, Vol. 3, pt. 1, Ed. C. M. Herzfeld. New York: Reinhold, p. 581.

(17) Kelly, Raymond L. Vacuum Ultraviolet Emission Lines (Below 2000 Angstroms). Stanford Research Institute: Menlo Park, California. UCRL 5612 (1959).

(18) Meek, J. M. and J. D. Craggs. Electrical Breakdown of Gases. Oxford: Clarendon Press, [illegible].

(19) Moore, C. E. "Atomic Energy Levels." Nat'l. Bur. Std. (U.S.), Circular 467, Vol. 1, (1949).

(20) Nagler, R. G. Temperature: Its Measurement and Control in Science and Industry, Vol. 3, pt. 1, Ed. C. M. Herzfeld. New York: Reinhold, (1962), p. 643.

(21) Paschen, F. "Die Funkenspektren des Aluminium. I. Teil." Annalen der Physik, 4 Folge, Band 71, (1923), p. 142.

(22) Paschen, F. "Erweiterung der Spektren Al II, Mg. I, Be I, und Al I." Annalen der Physik, 5 Folge, Band 12, (1932), p. 509.

(23) Penkin, N. P., and L. N. Shabanova. "Oscillator Strengths of the Al I and Ga I Spectral Lines." Optics and Spectroscopy (USA), Vol. 18, No. 5, (1964), p. 504.

(24) Perry, Larry J. "A Model and Calculations for the Properties of Laser Induced Plasmas." (Unpublished Ph.D. Thesis, Oklahoma State University, 1970).

(25) Perry, Larry J. "Design and Construction of a Twin-Ruby Laser." (Unpublished M.S. thesis, Oklahoma State University, 1967).

(26) Sawyer, R. A., und F. Paschen. "Das Erste Funkenspektrum des Aluminiums Al II." Annalen der Physik, 4 Folge, Band 84, (1927), p. 1.

(27) Selwyn, E. W. H. "Arc Spectra in the Region 1600-2100." Proceedings of the Physical Society, Vol. 41, pt. 2, No. 229, (June 15, 1929), p. 392.

(28) Soderqvist, J. "Die Spektren Mq. IV and Al V im Extremen Ultra violett." Zeitschrift fur Physik, Band 76, (1932), p. 756.

(29) Soderqvist, J. "Die Spektren Na IV, Mg. V, Al VI, und Mg. III, Al IV im Extremen Ultraviolett." Zeitschrift fur Physik, Band 79, (1932), p. 634.

(30) Soderqvist, J. "Vankuumfunkenspektren Der Elemente Natrium, Magnesium, Aluminium, und Silicium." Nova Acta Regiae Societatis Scientiarum Upsaliensis, Ser. IV, Vol. 9, No. 7, (Uppsala, 1934).

(31) Stratton, T. F. Temperature: Its Measurement and Control in Science and Industry, Vol. 3, pt. 1, Ed. C. M. Herzfeld. New York: Reinhold, (1962), p. 663.

(32) Vainshtein, L. A. "Calculation of Wave Functions and Oscillator Strengths of Complex Atoms." Transactions of the P. N. Lebqdev Physics Institute, Vol. XV, (1962), pt. 1. (Authorized translation from the Russian.)

(33) Varsavsky, C. M. "Some Atomic Parameters For Ultraviolet Lines." Astrophysical Journal, Supplement, Ser. 6, No. 53, (1961) p. 75.

(34) Willis, H. W. "Quadrupole Mass Filter Design and Construction for Plasma Ion Analysis." (M.S. Thesis, Oklahoma State University, 1969).

(35) Zumstein, R. V. "Wave-length Standards in the Spectra of Aluminum, Silicon and Bismuth in the Schumann Region." Physical Review, Vol. 38, (December 15, 1931), p. 2214.

APPENDIX A

THE SPECTROGRAPH AND CALCULATION OF WAVELENGTHS

The basic spectrograph was designed by my advisor, F. C. Todd. The film changer and the entrance slit was designed by H. G. Gurney. The devise was assembled and the first, fuzzy spectra was obtained by R. D. Payne. The design employs a concave grating in a Rowland mounting. To obtain a maximum of intensity and separation in the far ultra-violet, the light is incident on the grating at near grazing incidence. The entire optical path is enclosed in a high vacuum chamber.

The Grating Equation

Light of wavelength, λ, incidence on the grating at an angle D with respect to the normal to the grating, is diffracted so it makes an angle E with respect to the normal, as shown in Figure 6. The angle E can be found by Equation 1,

$$(1)\quad \lambda = 1/e\,(\sin D - \sin E),$$

where e is the grating constant.

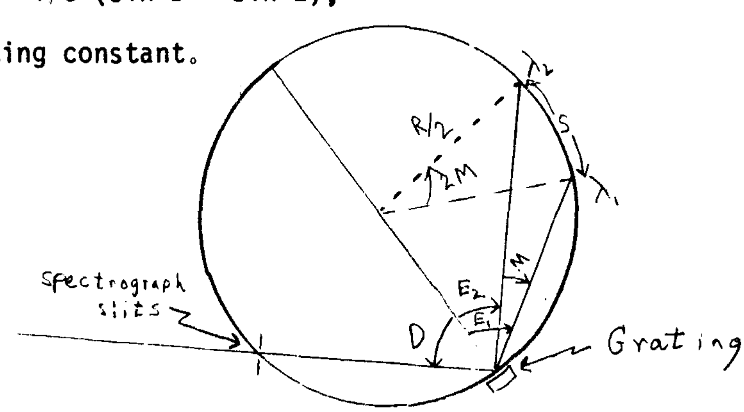

Figure 6. Diagram of a Concave Grating in a Rowland Mounting.

Determining the Angle of Incidence

The angle of incidence, D, may be determined if any two spectral lines are identified. For two known wavelengths, λ_1 and λ_2,

$$(2)\quad \lambda_1 = 1/e\ (\sin D - \sin E_1)$$

and

$$\lambda_2 = 1/e\ (\sin D - \sin E_2)$$

From Figure 1, a relation for the angles E_1 and E_2 is

$$(3)\quad E_1 = E_2 + M,$$

where, by a theorem in plane geometry, M is half of the angle that is subtended by the arc which joins the focus point of λ_1 and λ_2.

Subtract equation (2) from equation (1)

$$(4)\quad e\lambda_1 - e\lambda_2 = \sin E_2 - \sin E_1$$

and by substituting from equation (3)

$$e\lambda_1 - e\lambda_2 = \sin E_2 - \sin (E_2 + M)$$

Use the well known, trigonometry relations to obtain

$$(5)\quad e\lambda_1 - e\lambda_2 = \sin E_2(1-\cos M) - \cos E_2 \sin M$$

$$= (1-\cos M) \sin E_2 - \sin M\ (\sqrt{1-\sin^2 E_2})$$

For simplification, the following definations are introduced:

$$F = e\lambda$$

$$Z = \cos M$$

$$Y = \sin M$$

and $\quad X = \sin E_2$

With these substitutions,

$$(6)\quad F_1 - F_2 = (1-Z)\ X - Y\ (\sqrt{1-X^2})$$

which may be written as

$$(7)\quad (F_2 - F_1) + (1-Z)\ X = Y\ (\sqrt{1-X^2})$$

Square both sides of this equation and obtain

$$(F_2-F_1)^2 + (1-Z)^2 X^2 + 2(F_2-F_1)(1-Z) X = Y^2(1-X^2)$$

which may be rearranged into the following form.

(8) $\left((1-Z)^2 + Y^2\right) X^2 + 2(F_2-F_1)(1-Z) X + (F_2-F_1)^2 - Y^2 = 0$

Identifying the quantities

(9) $A = (1-Z)^2 + Y^2$

$B = 2(F_2-F_1)(1-Z)$

$C = (F_2-F_1)^2 - Y^2$

Equation (8) is the familiar quadratic equation.

(10) $AX^2 + BX + C = 0$

As λ_1 and λ_2 are known, and M is easily determined by measuring the arc length on the film, equation (10) may be solved for X.

Return to equations (2) and recall that $X = \sin E_2$.

(11) $\sin D = e\lambda_2 + X$

or

(12) $D = \arcsin(e\lambda_2 + X)$.

Identifying Spectral Lines

When the angle of incidence, D, is known, the wavelength of any of the spectral lines may be found. There are two ways to accomplish this. First, obtain the arc length on the Rowland circle from the center of the grating to the line, and from this length, compute the angle, equation (1). The second method assumes that at least one wavelength is already known. From the known (or reference) wavelength and from the unknown wavelength, equation (1) gives

(13) $e\lambda_r = \sin D - \sin E_r$

and

$e\lambda = \sin D - \sin E$

The first of these equations is solved for E_r. Subtract equation (13) from the unnumbered equation that follows it

$(\lambda - \lambda_r)e = \sin E_r - \sin E$

or

(14) $\lambda = \lambda_r + 1/e\,[\sin E_r - \sin E]$

Proceed as in calculating the angle, D,

(15) $E = E_r - M$

Substitute equation (15) in equation (14)to obtain

(16) $\lambda = \lambda_r + 1/e\,[\sin E_r - \sin (E_r - M)]$.

Since R is the radius of curvature of the grating and <u>s</u> is the arc length that separates the two lines, the angle M is

(17) $M = s/R$

The unknown wavelength is calculated from equation (16).

This latter method is employed rather than the one which is mentioned earlier. It is believed that the arc length may be found more accurately than the distance to the center of the grating. There is too large an uncertainty in determining the arc length from the center of the grating to the end of the sector where the film was placed and in determining the point on the film which corresponds to the end of the sector.

Using the lines 160.073 and 161.686 angstroms and their second order lines as the known wavelengths, the angle of incidence, D, was calculated as 85.63 degrees. The line 160.073 angstroms was used as the reference wavelength, for which E_r=78.01 degrees. The grating constant, ϵ, is 1.1811×10^5 mm^{-1}.

APPENDIX B

STRONG EMISSION LINES OF ALUMINUM

In the following tables are listed the stronger lines of the aluminum ions Al I through Al VIII. In each table, in this order, are listed the wavelength, the wave number, the term combination, and relative intensity for each strong line. When more than one reference is available the relative intensity from each is listed. It should be noted that differences in the numerical intensity reported may arise from the use of different intensity scales. In many instances the method of determining the intensity is not defined. In any case conversion from one scale to another is very difficult without the original data. In some cases the differences are real with one author reporting line _A_ stronger than line _B_ and another author reporting the opposite. An example of this is the 2513 and 2373 angstrom lines of the Al I table. Except for specific cases, which will be noted, the remainder of the information is taken from the most recent article.

Not all lines identified for a specific ion by the references are listed. Only the lines detectable in the first or second order on the available equipment are included. In addition, lines too faint to be easily detected are not listed.

ALUMINUM I

Most of the Al I lines are detectable in the first order on available equipment. The minimum relative intensity is taken as 6, as the listing is quite large. The lines of wavelength greater than 10,500 angstroms are beyond the range of available spectrographs, and are the only lines not detectable in the first order on available equipment.

The information is taken from a 1962 article by K. B. S. Erikson and H. B. S. Isberg except for four lines listed in a 1932 article by F. Paschen. Intensities have also been taken from the article by Paschen. Erikson and Isberg have revised some of the term designations used by Paschen. 3d' ^2F, 4d' ^2D, 4d' ^2F and 5d' ^2D, replace 5s' ^2P, 4d' ^2P, 5s' ^2P, and 5d' ^2F respectively. The term 3d' ^2P was discarded upon identification of the level 5s' $^4P_{2\frac{1}{2}}$.

The notation and information is from the 1962 article, with the exceptions as noted above. For other ions the notation used is that given in the 1949 work by C. E. Moore.

Al I has all 13 electrons, which in the ground state have the configuration $1s^2 2s^2 2p^6 3s^2 3p - {}^2P^o_{\frac{1}{2}}$. The ionization potential is 5.984 electron volts or $(48278.37 \pm 0.02)\ cm^{-1}$.

ALUMINUM II

All Al II lines listed are detectable in the first order on available equipment. The lower limit for relative intensity is taken as 5.

The listings for Al II are quite long. The most complete listing is from a 1927 article by R. A. Sawyer and F. Paschen. A 1932 article by Paschen lists some improved values. Shenstone and Russell suggested some revised term designations in a 1932 article. The newer designations are used in the work by C. E. Moore and are used here.

Al II has 12 remaining electrons which in the ground state have the configuration $1s^2 2s^2 2p^6 3s^2 - {}^1S_0$. The ionization potential is 18.823 electron volts or 151860.4 ± 0.5 cm^{-1}.

ALUMINUM III

The lines listed for Al III are all detectable in the first order available equipment. Only the stronger lines of relative intensity 5 or greater are listed.

The information is mainly from a 1923 article by F. Paschen. Some lines and terms not reported in that article are from a 1928 article by Eric Ekefors.

Al III has 11 electrons remaining which in the ground state have the configuration $1s^2 2s^2 2p^6 3s\ {}^2S_{1/2}$. The ionization potential is 28.44 electron volts or 229453.99 cm^{-1}.

ALUMINUM IV

The listings for Al IV are not as extensive as that for the other species. The list being short, the minimum relative intensity for the stronger lines has been set at 2.

The information is taken from a 1934 article by Jonas Soderqvist, with a few exceptions. The LS-coupling term designations used by Soderqvist have been replaced with the jl-coupling notations used in the work by C. E. Moore, as suggested by G. Racah. Moore points out; however, that three configurations have been found to be closer to

LS-coupling than to jl-coupling. They are $2p^5$ 3s, $2p^5$ 3p, and $2p^5$ 3d.

Al IV has 10 electrons left in the ground state configurations $1s^2 2s^2 2p^6$ - $^1S_0$. The ionization potential is 119.96 electron volts or 967783 cm^{-1}.

ALUMINUM V

A large number of Al V lines are detectable in the first order on the available equipment. The lines of relative intensity 5 or greater are listed. Lines detectable in the second order only are listed if relative intensity is 10 or greater. Additional lines which have been detected on the spectra discussed in this report are listed.

The information is taken principally from a 1948 article by Eric Ferner. Some lines of wavelength greater than 137 angstroms are not reported in this article but are reported in the 1934 article by Jonas Soderqvist. The ionization potential is from some unpublished material by H. A. Robinson, quoted in the work by C. E. Moore.

Al V has 9 remaining electrons which in the ground state have the configuration $1s^2 2s^2 sp^5$ - $^2P^o_{1\frac{1}{2}}$. The ionization potential is 153.77 volts or 1240600 cm^{-1}.

ALUMINUM VI

Several Al VI lines are detectable in the first order on available instruments. Above the lower limit of the instruments, 100 angstroms, we list lines of minimum relative intensity 5. Other lines which have been detected in spectra taken by this instrument are also listed. Lines of minimum relative intensity 10 which are detectable in the second order are also listed.

Most of the information is taken from a 1948 article by Eric Ferner. Lines above 113 angstroms are taken from listings in a 1934 article by Jonas Soderqvist. Several lines are listed in both articles.

Al VI has 8 electrons remaining in the ground state configuration $1s^2 2s^2 2p^4 - {}^3P_2$. The ionization potential is 190.42 electron volts or 1536300 cm^{-1}.

ALUMINUM VII

Few Al VII lines are detectable in the first order on the presently available equipment. Lines of minimum relative intensity 2 which are detectable in the first order are listed. Lines detectable in the second order of minimum relative intensity 10 are also listed.

The information has been taken from a 1948 article by Eric Ferner except for the lines detectable in the first order. The information for the first order lines are from a 1934 article by Jonas Soderqvist.

Al VII has 7 electrons remaining in the ground state configuration $1s^2 2s^2 2p^3 - {}^4S^o_{1\frac{1}{2}}$. The ionization potential is 241.93 electron volts or 1951630 cm^{-1}.

ALUMINUM VIII

No first order Al VIII line would be detectable using the presently available equipment. The very strong lines which could be detected in the second order on this equipment, however, are listed. The minimum relative intensity has been placed at 10. If equipment becomes available for first order detection a lower intensity should be selected and the listings expanded.

The information is taken from a 1948 article by Eric Ferner.

Al VIII has 6 electrons and in the ground state has the configur-acions $1s^2 2s^2 2p^2$ - $^3P_0$. The ionization potential is 285.13 elactron volts or, 2300390 cm^{-1}.

TABLE IV

STRONG EMISSION LINES OF Al I

Wave Length	Wave Number	Term Combination	Intensity E&I	Intensity P
21163.75	4723.772	4p $^2P_{1\frac{1}{2}}$ - 5s $^2S_{\frac{1}{2}}$	13	
21093.04	4739.606	4p $^2P_{\frac{1}{2}}$ - 5s $^2S_{\frac{1}{2}}$	12	
16763.36	5963.763	4p $^2P_{1\frac{1}{2}}$ - 4d $^2D_{1\frac{1}{2}}$	9	
16750.56	5968.318	4p $^2P_{1\frac{1}{2}}$ - 4d $^2D_{2\frac{1}{2}}$	12	
16718.96	5979.601	4p $^2P_{\frac{1}{2}}$ - 4d $^2D_{1\frac{1}{2}}$	11	
13150.76	7602.047	4s $^2S_{\frac{1}{2}}$ - 4p $^2P_{\frac{1}{2}}$	14	
13123.41	7617.888	4s $^2S_{\frac{1}{2}}$ - 4p $^2P_{1\frac{1}{2}}$	15	
11254.881	8882.602	3d $^2D_{2\frac{1}{2}}$ - 4f $^2F_{3\frac{1}{2}}$	15	
11253.190	8883.936	3d $^2D_{1\frac{1}{2}}$ - 4f $^2F_{2\frac{1}{2}}$	14	
10891.733	9178.761	4p $^2P_{1\frac{1}{2}}$ - 6s $^2S_{\frac{1}{2}}$	11	
10872.975	9194.596	4p $^2P_{\frac{1}{2}}$ - 6s $^2S_{\frac{1}{2}}$	10	
10782.045	9272.138	4p $^2P_{1\frac{1}{2}}$ - 5d $^2D_{2\frac{1}{2}}$	9	
10768.364	9283.919	4p $^2P_{\frac{1}{2}}$ - 5d $^2D_{1\frac{1}{2}}$	8	
9139.950	10937.98	$3p^2$ $^2P_{1\frac{1}{2}}$ - 3d' $^2D_{2\frac{1}{2}}$	6	
8823.555	11216.613	4p $^2P_{1\frac{1}{2}}$ - 6d $^2D_{2\frac{1}{2}}$	9	
8912.900	11216.613	4p $^2P_{\frac{1}{2}}$ - 6d $^2D_{1\frac{1}{2}}$	7	
8841.277	11307.478	4p $^2P_{1\frac{1}{2}}$ - 7s $^2S_{\frac{1}{2}}$	10	
8828.909	11323.319	4p $^2P_{\frac{1}{2}}$ - 7s $^2S_{\frac{1}{2}}$	8	

TABLE IV (Continued)

Wave Length	Wave Number	Term Combination	Intensity E&I	Intensity P
8773.896	11394.316	3d $^2D_{2\frac{1}{2}}$ - 5f $^2F_{3\frac{1}{2}}$	14	
8772.866	11395.654	3d $^2D_{1\frac{1}{2}}$ - 5f $^2F_{2\frac{1}{2}}$	13	
8075.353	12379.955	4p $^2P_{1\frac{1}{2}}$ - 7d $^2D_{2\frac{1}{2}}$	8	
8065.968	12394.360	4p $^2P_{\frac{1}{2}}$ - 7d $^2D_{1\frac{1}{2}}$	6	
8003.186	12491.588	4p $^2P_{1\frac{1}{2}}$ - 8s $^2S_{\frac{1}{2}}$	7	
7836.134	12757.885	3d $^2D_{2\frac{1}{2}}$ - 6f ^2F	12	
7835.309	12759.228	3d $^2D_{1\frac{1}{2}}$ - 6f ^2F	11	
7614.820	13128.673	4p $^2P_{1\frac{1}{2}}$ - 8d $^2D_{2\frac{1}{2}}$	7	
7362.297	13578.977	3d $^2D_{2\frac{1}{2}}$ - 7f ^2F	9	
7361.568	13580.322	3d $^2D_{1\frac{1}{2}}$ - 7f ^2F	8	
7084.644	14111.145	3d $^2D_{2\frac{1}{2}}$ - 8f ^2F	6	
6698.673	14924.209	4s $^2S_{\frac{1}{2}}$ - 5p $^2P_{\frac{1}{2}}$	11	
6696.023	14930.116	4s $^2S_{\frac{1}{2}}$ - 5p $^2P_{1\frac{1}{2}}$	13	
5557.948	17987.257	4s $^2S_{\frac{1}{2}}$ - 6p $^2P_{\frac{1}{2}}$	8	
5557.053	17990.121	4s $^2S_{\frac{1}{2}}$ - 6p $^2P_{1\frac{1}{2}}$	10	
5107.520	19573.519	4s $^2S_{\frac{1}{2}}$ - 7p $^2P_{1\frac{1}{2}}$	6	
3961.5200	25235.695	3p $^2P_{1\frac{1}{2}}$ - 4s $^2S_{\frac{1}{2}}$	26	
3944.0058	25354.757	3p $^2P_{\frac{1}{2}}$ - 4s $^2S_{\frac{1}{2}}$	24	
3479.806	28729.01	4d $^2D_{2\frac{1}{2}}$ - 3d' $^2D_{2\frac{1}{2}}$	5	6
3458.216	28908.36	3p $^2P_{1\frac{1}{2}}$ - $3p^2$ $^4P_{\frac{1}{2}}$	6	8
3444.865	29020.40	3p $^2P_{\frac{1}{2}}$ - $3p^2$ $^4P_{\frac{1}{2}}$	6	7
3443.640	29030.72	3p $^2P_{1\frac{1}{2}}$ - $3p^2$ $^4P_{2\frac{1}{2}}$	9	10
3439.347	29066.96	3p $^2P_{\frac{1}{2}}$ - $3p^2$ $^4P_{1\frac{1}{2}}$	6	8

TABLE IV (Continued)

Wave Length	Wave Number	Term Combination	Intensity F&I	Intensity P
3092.8386	32323.374	3p $^2P_{1\frac{1}{2}}$ - 3d $^2D_{1\frac{1}{2}}$	20	
3092.7099	32314.719	3p $^2P_{1\frac{1}{2}}$ - 3d $^2D_{2\frac{1}{2}}$	26	
3082.1529	32435.433	3p $^2P_{\frac{1}{2}}$ - 3d $^2D_{1\frac{1}{2}}$	24	
3064.290	32624.50	$3p^2$ $^4P_{1\frac{1}{2}}$ - 4s' $^4P_{\frac{1}{2}}$	7	5
3057.144	32700.76	$3p^2$ $^4P_{2\frac{1}{2}}$ - 4s' $^4P_{2\frac{1}{2}}$	14	10
3050.073	32776.57	$3p^2$ $^4P_{1\frac{1}{2}}$ - 4s' $^4P_{2\frac{1}{2}}$	13	9
2840.099	35199.69	3d $^2D_{1\frac{1}{2}}$ - 3d' $^2D_{1\frac{1}{2}}$	7	10
2837.963	35226.18	3d $^2D_{1\frac{1}{2}}$ - 3d' $^2D_{2\frac{1}{2}}$	7	12
2740.980	36472.51	5d $^2D_{2\frac{1}{2}}$ - 4d' $^2F_{3\frac{1}{2}}$	4	7
2657.406	37619.49	4d $^2D_{2\frac{1}{2}}$ - 4d' $^2D_{2\frac{1}{2}}$	3	6
2647.49	37760.4	$^4D_{3\frac{1}{2}}$ - $^4F_{4\frac{1}{2}}$		6
2519.22	39682.85	4d $^2D_{1\frac{1}{2}}$ - 4d' $^2F_{2\frac{1}{2}}$	4	6
2513.305	39776.27	4d $^2D_{2\frac{1}{2}}$ - 4d' $^2F_{3\frac{1}{2}}$	5	9
2373.571	42117.75	$3p^2$ $^4P_{2\frac{1}{2}}$ - 3d' $^4D_{2\frac{1}{2}}$	8	6
2372.070	42143.59	$3p^2$ $^4P_{2\frac{1}{2}}$ - 3d' $^4D_{3\frac{1}{2}}$	10	10
2370.726	42168.29	$3p^2$ $^4P_{1\frac{1}{2}}$ - 3d' $^4D_{\frac{1}{2}}$	6	2
2370.225	42177.21	$3p^2$ $^4P_{1\frac{1}{2}}$ - 3d' $^4D_{1\frac{1}{2}}$	9	6
2369.304	42193.60	$3p^2$ $^4P_{1\frac{1}{2}}$ - 3d' $^4D_{2\frac{1}{2}}$	10	8
2368.112	42214.84	$3p^2$ $^4P_{\frac{1}{2}}$ - 3d' $^4D_{\frac{1}{2}}$	8	5
2367.611	42223.77	$3p^2$ $^4P_{\frac{1}{2}}$ - 3d' $^4D_{1\frac{1}{2}}$	8	5
2321.562	43061.22	$3p^2$ $^4P_{2\frac{1}{2}}$ - 3d' $^4P_{2\frac{1}{2}}$	9	8
2317.482	43137.03	$3p^2$ $^4P_{1\frac{1}{2}}$ - 3d' $^4P_{2\frac{1}{2}}$	7	5

TABLE IV (Continued)

Wave Length	Wave Number	Term Combination	Intensity E&I	Intensity F
2313.526	43210.78	$3p^2\ {}^4P_{1\frac{1}{2}} - 3d'\ {}^4P_{\frac{1}{2}}$	6	4
2266.014	44116.71	$3d\ {}^2D_{2\frac{1}{2}} - 4d'\ {}^2D_{2\frac{1}{2}}$	3	7
2180.996	45836.26	$3p^2\ {}^4P_{2\frac{1}{2}} - 5s'\ {}^4P_{2\frac{1}{2}}$	5	8
2177.396	45912.04	$3p^2\ {}^4P_{1\frac{1}{2}} - 5s'\ {}^4P_{2\frac{1}{2}}$	4	6
2160.383	46273.55	$3d\ {}^2D_{2\frac{1}{2}} - 4d'\ {}^2F_{3\frac{1}{2}}$	3	6
1769.19		$3p\ {}^2P_2 - 3p^2\ {}^2P_1$		1
1766.41		$3p\ {}^2P_2 - 3p^2\ {}^2P_2$		2
1762.97		$3p\ {}^2P_1 - 3p^2\ {}^2P_1$		1

TABLE V

STRONG EMISSION LINES OF Al II

Wave Length	Wave Number	Term Combination	Intensity S&P	Intensity P
7042.06	14196.5	4s $^3S_1$ - 4p $^3P^o_2$	5	
6335.70	15779.2	3d $^1D_2$ - 5p $^1P^o_1$	5	
6243.35	16012.6	4p $^3P^o_2$ - 4d $^3D_3$	10	
6231.76	16042.4	4p $^3P^o_1$ - 4d $^3D_2$	7	
6226.19	16042.4	4p $^3P^o_1$ - 4d $^3D_1$	5	
6006.38	16644.4	5p $^3P^o_2$ - 7d ^3D	6	
5972.05	16740.0	5p $^1P^o_1$ - 7d $^1D_2$	5	
5853.62	17078.7	4d $^3D_3$ - 6f $^3F^o_4$	5	
5593.23	17873.8	4p $^1P^o_1$ - 4d $^1D_2$	10	
5371.84	18610.4	4d $^3D_{3,2}$ - 7p $^3P^o$	6	
5316.07	18805.7	5p $^3P^o_2$ - 9s $^3S_1$	7	
5312.32	18818.9	5p $^3P^o_1$ - 9s $^3S_1$	5	
5283.77	18920.6	5p $^3P^o_2$ - 8d ^3D	8	
5285.85	18913.2	5p $^1P^o_1$ - 8d $^1D_2$	6	
5280.21	18933.4	5p $^3P^o_1$ - 8d ^3D	6	
4902.77	20391.0	5p $^3P^o_2$ -10s $^3S_1$	5	
4898.76	20407.7	5p $^1P^o_1$ - 9d $^1D_2$	5	
4666.8	21422	5p $^1P^o_1$ -11s $^1S_0$	11	

TABLE V (Continued)

Wave Length	Wave Number	Term Combination		Intensity S&P	P
4588.194	21788.97	4d $^3D_2$	- 7f $^3F^o_3$	5	
4585.820	21800.25	4d $^3D_3$	- 7f $^3F^o_4$	6	
4227.493	23648.02	4d $^3D_2$	- 8f $^3F^o_3$	5	
4226.812	23651.83	4d $^3D_3$	- 8f $^3F^o_4$	6	
4026.5	24828.5	3d $^1D_2$	- 6p $^1P^o_1$	5	
3995.860	25018.83	4d $^3D_3$	- 9f $^3F^o_4$	5	
3900.680	25629.32	3p $^1P^o_1$	- $3p^2$ $^1D_2$	10	
3655.000	27352.00	4p $^3P^o_2$	- 5d $^3D_3$	8	
3651.064	27381.49	4p $^3P^o_1$	- 5d $^3D_2$	6	
3428.916	29155.39	3d $^1D_2$	- 6f $^1F^o_3$		
3074.665	32514.08	3d $^1D_2$	- 7f $^1F^o_3$	6	
3057.155	32700.66			10	
3050.073	32776.58			8	
3041.278	32871.37	3d $^1D_2$	- 8p $^1P^o_1$	6	
2868.52	34851.0	3d $^1D_2$	- 9p $^1P^o_1$	9	
2816.179	35498.67	3p $^1P^o_1$	- 4s $^1S_0$	20	
2669.166	37453.76	$3s^2$ $^1S_0$	- 3p $^3P^o_1$	10	
2637.696	37900.57	3d $^3D_3$	- 5f $^3F^o_4$	5	
2631.553	37989.07	$3p^2$ $^1D_2$	- 4f $^1F^o_3$	7	
2627.68	38045.1	3d $^1D_2$	-11f $^1F^o_3$	7	
2597.18	38491.9	3d $^1D_2$	-12p $^1P^o_1$	6	
2586.95	38644.1	3d $^1D_2$	-12f $^1F^o_3$	6	

TABLE V (Continued)

Wave Length	Wave Number	Term Combination		Intensity S&P	P
2557.71	39085.7	4p $^3P^o_1$	- 9s $^3S_1$	5	
2552.12	39171.2	4p $^3P^o_2$	- 8d ^3D	5	
2321.56	43061.32			6	
2099.68	47611.3	4s $^1S_0$	- 8p $^1P^o_1$	5	
2095.2	47713	3d $^3D_1$	- 7f $^3F_2$	5	
2094.8	47722	3d $^3D_2$	- 7f $^3F^o_3$	5.5	
2094.3	47734	3d $^3D_3$	- 7f $^3F^o_4$	6	
2087.0	47901	3p $^3P^o_2$	- 3p^2 $^1D_2$	5	
2016.91	49581	4s $^1S_0$	- 9p $^1P^o_1$	10	
1990.53	50238	3p $^1P^o_1$	- 3d $^1D_2$	7	
1962.67	50951	4s $^1S_0$	-10p $^1P^o_1$	7	
1945.35	51404			5	
1939.30	51565.0	3p^2 $^3P_2$	- 4s $^3P^o_1$	5	5
1934.75	51686.3	3p^2 $^3P_1$	- 4s $^3P^o_1$	10	10
1934.54	51692.0	3p^2 $^3P_2$	- 4s $^3P^o_2$	10	10
1932.43	52748.2	2p^2 $^3P_0$	- 4s $^3P^o_1$		
1930.03	51812.5	3p^2 $^3P_1$	- 4s $^3P^o_2$	5	5
1910.91	52331.1	3p^2 $^3P_2$	- 3d $^3P^o_2$	5	5
1862.38	53694.6	3p $^3P^o_2$	- 4s $^3S_1$	15	
1858.08	53819.1	3p $^3P^o_1$	- 4s $^3S_1$	10	
1855.97	53880.1	3p $^3P^o_0$	- 4s $^3S_1$	8	8
1834.82	54501.2	4s $^3S_1$	- 4s $^3P^o_0$	6	6

TABLE V (Continued)

Wave Length	Wave Number	Term Combination	Intensity S&P	Intensity P
1832.85	54559.9	$4s\ ^3S_1 - 4s\ ^3P^o_1$	8	8
1828.59	54687.0	$4s\ ^3S_1 - 4s\ ^3P^o_2$	10	10
1767.76	56568.8	$3p\ ^3P^o_2 - 3p^2\ ^3P_1$	7	
1764.01	56689.0	$3p\ ^3P^o_2 - 3p^2\ ^3P_2$	10	
1763.85	56694.0	$3p\ ^3P^o_1 - 3p^2\ ^3P_1$	8	
1762.00	56753.5	$3p\ ^3P^o_0 - 3p^2\ ^3P^o_0$	5	
1760.15	56813.3	$3p\ ^3P^o_1 - 3p^2\ ^3P_2$	7	
1750.56	57125	$3p^2\ ^1D_2 - 7f\ ^1F^o_3$	6	
1739.64	57483	$3p^2\ ^1D_2 - 8p\ ^1P^o_1$	5	
1725.01	57971	$3p\ ^3P^o_2 - 3d\ ^3D_{3,2,1}$	15	
1721.31	58095	$3p\ ^3P^o_1 - 3d\ ^2D_{3,2,1}$	10	
1719.43	58159	$3p\ ^3P^o_0 - 3d\ ^3D_{3,2,1}$	8	
1686.19	59305	$3p^2\ ^1D_2 - 8f\ ^1F_3$	5	
1681.78	59461	$3p^2\ ^1D_2 - 9p\ ^1P^o_1$	5	
1670.81	59851	$3s^2\ ^1S_0 - 3p\ ^1P^o_1$	15	
1644.78	60798	$3p^2\ ^1D_2 - 9f\ ^1F^o_3$	5	
1644.15	60821	$3p^2\ ^1D_2 - 10p\ ^1P^o_1$	5	
1539.74	64946	$3p\ ^1P^o_1 - 4d\ ^1D_2$	10	
1350.15	74066	$3p\ ^1P^o_1 - 5d\ ^1D_2$	6	
1191.86	83902	$3p\ ^3P^o_2 - 4d\ ^3D_1$	5	

TABLE VI

STRONG EMISSION LINES OF Al III

Wave Length	Wave Number	Term Combination	Intensity P	Intensity E
5722.65	17469.57	4s $^{2}S_{\frac{1}{2}}$ - 4p $^{2}P^{o}_{\frac{1}{2}}$	6	
5696.47	17549.87	4s $^{2}S_{\frac{1}{2}}$ - 4p $^{2}P^{o}_{1\frac{1}{2}}$	8	
5163.90	19359.82	5g ^{2}G - 7h $^{2}H^{o}$	7	
5150.86	19406.83	5f $^{2}F^{o}_{2\frac{1}{2}}$ - 7g ^{2}G	6	
4701.65	21263.98	4f $^{2}F^{o}_{2\frac{1}{2}}$ - 5d ^{2}D	6	
4529.176	22072.88	4p $^{2}P^{o}_{1\frac{1}{2}}$ - 4d $^{2}D_{2\frac{1}{2}}$	6	
3601.623	27757.35	3d $^{2}D_{2\frac{1}{2}}$ - 4p $^{2}P^{o}_{1\frac{1}{2}}$	6	
2907.05	34389.08	4f $2F^{o}_{3\frac{1}{2}}$ - 6g ^{2}G	10	
2762.815	36184.30	4d $^{2}D_{2\frac{1}{2}}$ - 6f $^{2}F^{o}$	9	
1935.83	51657.43	3d $^{2}D_{2\frac{1}{2}}$ - 4f $^{2}F^{o}_{3\frac{1}{2}}$	10	
1862.749	53684.1	3s $^{2}S_{\frac{1}{2}}$ - 3p $^{2}P^{o}_{\frac{1}{2}}$	10	10
1854.715	53916.6	3s $^{2}S_{\frac{1}{2}}$ - 3p $^{2}P^{o}_{1\frac{1}{2}}$	10	10
1605.776	62275.2	2p $^{2}P^{o}_{\frac{1}{2}}$ - 3d $^{2}D_{1\frac{1}{2}}$	8	7
1611.849	62040.6	3p $^{2}P^{o}_{1\frac{1}{2}}$ - 3d $^{2}D_{1\frac{1}{2}}$	8	9
1384.144	72246.8	3p $^{2}P^{o}_{1\frac{1}{2}}$ - 4s $^{2}S_{\frac{1}{2}}$	5	8
1379.670	72481.1	3p $^{2}P^{o}_{\frac{1}{2}}$ - 4s $^{2}S_{\frac{1}{2}}$		6
893.905	111868.7	3p $^{2}P^{o}_{1\frac{1}{2}}$ - 3d $^{2}D_{2\frac{1}{2}}$		5
856.768	116717.7	3p $^{2}P^{o}_{1\frac{1}{2}}$ - 5s $^{2}S_{\frac{1}{2}}$		5

MISSING

PRECEDING PAGE B[redacted]K NOT FILMED.

TABLE VI (Continued)

Wave Length	Wave Number	Term Combination	Intensity P	Intensity E
695.817	143716.0	$3s\ ^2S_{\frac{1}{2}} - 4p\ ^2P^o_{1\frac{1}{2}}$		5
560.390	178447.2	$3s\ ^2S_{\frac{1}{2}} - 5p\ ^2P^o_{\frac{1}{2},1\frac{1}{2}}$		7

TABLE VII

STRONG EMISSION LINES OF Al IV

Wave Length	Wave Number	Term Combination	Intensity
1639.00	61012.8	3s' $[\frac{1}{2}]^{o}_{1}$ - 3p $[1\frac{1}{2}]_{2}$	2
1584.45	63113.4	3s' $[\frac{1}{2}]^{o}_{1}$ - 3p' $[1\frac{1}{2}]_{2}$	2
1582.04	63209.5	3s $[1\frac{1}{2}]^{o}_{1}$ - 3p $[2\frac{1}{2}]_{2}$	3
1557.24	64216.2	3s $[1\frac{1}{2}]^{o}_{2}$ - 3p $[2\frac{1}{2}]_{3}$	5
1447.47	69086.1	3s $[1\frac{1}{2}]^{o}_{2}$ - 3p $[1\frac{1}{2}]_{2}$	2
1431.93	69835.8	3s $[1\frac{1}{2}]^{o}_{1}$ - 3p $[\frac{1}{2}]_{0}$	2
1404.72	71188.6	3s $[1\frac{1}{2}]^{o}_{2}$ - 3p' $[1\frac{1}{2}]_{2}$	2
1388.77	72006.2	3s $[1\frac{1}{2}]^{o}_{2}$ - 3p' $[\frac{1}{2}]_{1}$	2
1302.13	76797.2	3p' $[\frac{1}{2}]_{0}$ - 3d $[1\frac{1}{2}]^{o}_{1}$	2
1272.70	78573.1	3p $[1\frac{1}{2}]_{2}$ - 3d $[2\frac{1}{2}]^{o}_{3}$	3
1264.14	79105.2	3p' $[\frac{1}{2}]_{1}$ - 3d' $[1\frac{1}{2}]^{o}_{2}$	3
1257.58	79517.8	3p' $[1\frac{1}{2}]_{2}$ - 3d' $[2\frac{1}{2}]^{o}_{3}$	3
1248.76	80079.4	3p $[1\frac{1}{2}]_{1}$ - 3d' $[2\frac{1}{2}]^{o}_{2}$	2
1240.83	80591.2	3p $[2\frac{1}{2}]_{2}$ - 3d $[3\frac{1}{2}]^{o}_{3}$	3
1240.18	80633.5	3p $[1\frac{1}{2}]_{1}$ - 3d $[2\frac{1}{2}]^{o}_{2}$	2
1237.14	80831.6	3p $[2\frac{1}{2}]_{3}$ - 3d $[3\frac{1}{2}]^{o}_{4}$	4
1136.80	87966.2	3p $[\frac{1}{2}]_{1}$ - 3d $[\frac{1}{2}]^{o}_{1}$	3
1118.80	89381.5	3p $[\frac{1}{2}]_{1}$ - 3d $[1\frac{1}{2}]^{o}_{2}$	4

TABLE VII (Continued)

Wave Length	Wave Number	Term Combination	Intensity
161.686	618483	$2p^6\ ^1S_0 - 3s\ [1\frac{1}{2}]^o_1$	14
160.073	624715	$2p^6\ ^1S_0 - 3s'\ [\frac{1}{2}]^o_1$	16
131.652	759578	$2p^6\ ^1S_0 - 3d\ [\frac{1}{2}]^o_1$	3
130.403	766854	$2p^6\ ^1S_0 - 3d\ [1\frac{1}{2}]^o_1$	11
129.729	880838	$2p^6\ ^1S_0 - 3d'\ [1\frac{1}{2}]^o_1$	12
124.543	802936	$2p^6\ ^1S_0 - 4s\ [1\frac{1}{2}]^o_1$	6
124.034	806231	$2p^6\ ^1S_0 - 4s'\ [\frac{1}{2}]^o_1$	8
116.920	855286	$2p^6\ ^1S_0 - 4d\ [1\frac{1}{2}]^o_1$	5
116.459	858671	$2p^6\ ^1S_0 - 4d'\ [1\frac{1}{2}]^o_1$	7

TABLE VIII

STRONG EMISSION LINES OF Al V

Wave Length	Wave Number	Term Combination	Intensity F	Intensity S
281.397	355370	$2p^5\ {}^2P^o_{1/2} - 2p^6\ {}^2S_{1/2}$		14
278.699	358810	$2p^5\ {}^2P^o_{1\frac{1}{2}} - 2p^6\ {}^2S_{1/2}$		16
132.630	753977	$2p^5\ {}^2P^o_{1\frac{1}{2}} - 3s\ {}^4P_{1\frac{1}{2}}$	10	6
131.441	760798	$2p^5\ {}^2P^o_{1/2} - 3s\ {}^2P_{1\frac{1}{2}}$	20	9
131.003	763341	$2p^5\ {}^2P^o_{1/2} - 3s\ {}^2P_{1/2}$	20	10
130.848	764246	$2p^5\ {}^2P^o_{1\frac{1}{2}} - 3s\ {}^2P_{1\frac{1}{2}}$	20	12
130.413	766795	$2p^5\ {}^2P^o_{1\frac{1}{2}} - 3s\ {}^2P_{1/2}$	20	11
126.065	793242	$2p^5\ {}^2P^o_{1/2} - 3s'\ {}^2D_{1\frac{1}{2}}$	15	10
125.525	796654	$2p^5\ {}^2P^o_{1\frac{1}{2}} - 3s'\ {}^2D_{1\frac{1}{2}}$	15	12
118.500	843882	$2p^5\ {}^2P^o_{1\frac{1}{2}} - 3s''\ {}^2S_{1/2}$	10	6
108.707	919904	$2p^5\ {}^2P^o_{1\frac{1}{2}} - 3d\ {}^4D_{2\frac{1}{2}}$	6	4
108.462	921982	$2p^5\ {}^2P^o_{1/2} - 3d\ {}^2D_{1\frac{1}{2}}$	10	6
108.404	922475	$2p^5\ {}^2P^o_{1/2} - 3d\ {}^2P_{1/2}$	5	
108.385	922637	$2p^5\ {}^2P^o_{1\frac{1}{2}} - 3d\ {}^4P_{2\frac{1}{2}}$	10	6
108.112	924967	$2p^5\ {}^2P^o_{1/2} - 3d\ {}^2P_{1\frac{1}{2}}$	12	5
108.057	925438	$2p^5\ {}^2P^o_{1\frac{1}{2}} - 3d\ {}^2D_{1\frac{1}{2}}$	12	5
108.004	925892	$1p^5\ {}^2P^o_{1/2} - 3d\ {}^2P_{1/2}$	5	
107.945	926398	$2p^5\ {}^2P^o_{1\frac{1}{2}} - 3d\ {}^2D_{2\frac{1}{2}}$	20	6

TABLE VIII (Continued)

Wave Length	Wave Number	Term Combination	Intensity F	Intensity S
107.711	928410	$2p^5\ ^2P^o_{1\frac{1}{2}}$ - 3d $^2P_{1\frac{1}{2}}$	6	4
104.495	956983	$2p^5\ ^2P^o_{\frac{1}{2}}$ - 3d' $^2P_{\frac{1}{2}}$	8	3
104.447	957423	$2p^5\ ^2P^o_{\frac{1}{2}}$ - 3d' $^2S_{\frac{1}{2}}$	10	3
104.363	958194	$2p^5\ ^2P^o_{\frac{1}{2}}$ - 3d' $^2P_{1\frac{1}{2}}$	10	
104.180	959877	$2p^5\ ^2P^o_{\frac{1}{2}}$ - 3d' $^2D_{1\frac{1}{2}}$	14	4
104.121	960421	$2p^5\ ^2P^o_{1\frac{1}{2}}$ - 3d' $^2P_{\frac{1}{2}}$	12	3
104.073	960864	$2p^5\ ^2P^o_{1\frac{1}{2}}$ - 3d' $^2S_{\frac{1}{2}}$	10	6
103.881	962640	$2p^5\ ^2P^o_{1\frac{1}{2}}$ - 3d' $^2D_{2\frac{1}{2}}$	14	6
103.805	963345	$2p^5\ ^2P^o_{1\frac{1}{2}}$ - 3d' $^2D_{1\frac{1}{2}}$	10	5
99.290	1007150	$2p^5\ ^2P^o_{1\frac{1}{2}}$ - 3d'' $^2D_{2\frac{1}{2}}$	10	3
96.150	1040040	$2p^5\ ^2P^o_{\frac{1}{2}}$ - 4s' $^2D_{1\frac{1}{2}}$	1	4
93.955	1064340	$2p^5\ ^2P^o_{\frac{1}{2}}$ - 4d $^2P_{1\frac{1}{2}}$	6	3

TABLE IX

STRONG EMISSION LINES OF AL VI

Wave Length	Wave Number	Term Combination		Intensity F	S
312.241	320265	$2p^4\ ^3P_1$	$- 2p^5\ ^3P^o_2$		6
310.908	321639	$2p^4\ ^3P_0$	$- 2p^5\ ^3P^o_1$		6
309.852	322735	$2p^4\ ^3P_1$	$- 2p^5\ ^3P^o_1$		6
309.596	323002	$2p^4\ ^3P_2$	$- 2p^5\ ^3P^o_2$		8
308.560	324086	$2p^4\ ^3P_1$	$- 2p^5\ ^3P^o_0$		6
307.248	325470	$2p^4\ ^3P_2$	$- 2p^5\ ^3P^o_1$		7
275.350	363174	$2p^4\ ^1S_0$	$- 2p^5\ ^1P^o_1$		6
243.760	410240	$2p^4\ ^1D_2$	$- 2p^5\ ^1P^o_1$		12
113.437	881547	$2p^5\ ^3P^o_2$	$- 3s'''\ ^3P_2$	3	
109.843	910390	$2p^4\ ^3P_1$	$- 3s\ ^3S^o_1$	12	2
109.514	913125	$2p^4\ ^3P_2$	$- 3s\ ^3S^o_1$	20	3
107.620	929195	$2p^4\ ^1D_2$	$- 3s'\ ^1D^o_2$	14	5
104.466	957249	$2p^4\ ^3P_0$	$- 3s'\ ^3D^o_1$	8	
104.344	958368	$2p^4\ ^3P_1$	$- 3s'\ ^3D^o_{12}$	16	6
104.047	961104	$2p^4\ ^3P_2$	$- 3s'\ ^3D^o_{23}$	20	6
101.027	989834	$2p^4\ ^3P_0$	$- 3s''\ ^3P^o_1$	3	0
100.919	990894	$2p^4\ ^3P_1$	$- 3s''\ ^3P^o_{01}$	4	1
100.894	991139	$2p^4\ ^3P_1$	$- 3s''\ ^3P_2$	4	1

TABLE IX (Continued)

Wave Length	Wave Number	Term Combination		Intensity F	Intensity S
100.616	993878	$2p^4\ {}^3P_2$	$-\ 3s''\ {}^3P_2$	12	1
92.875	1076720	$2p^4\ {}^3P_0$	$-\ 3d\ {}^3D^o_1$	10	2
92.626	1079610	$2p^4\ {}^3P_2$	$-\ 3d\ {}^3D^o_3$	15	3
91.332	1094910	$2p^4\ {}^1D_2$	$-\ 3d'\ {}^1P^o_1$	10	0
90.858	1100620	$2p^4\ {}^1D_2$	$-\ 3d'\ {}^1D^o_2$	12	1
90.200	1108650	$2p^4\ {}^1D_2$	$-\ 3d'\ {}^1F^o_3$	20	2
88.376	1131530	$2p^4\ {}^3P_1$	$-\ 3d'\ {}^3D^o_{12}$	15	1
88.273	1132850	$2p^4\ {}^1D_2$	$-\ 3d''\ {}^1F^o_3$	15	
88.170	1134170	$2p^4\ {}^3P_2$	$-\ 3d'\ {}^3D^o_{23}$	20	2
87.655	1140840	$2p^4\ {}^3P_2$	$-\ 3d'\ {}^2P^o_2$	13	1
87.592	1141660	$2p^4\ {}^3P_2$	$-\ 3d'\ {}^3P_1$	10	0
85.515	1169390	$2p^4\ {}^3P_2$	$-\ 3d''\ {}^3D^o_3$	20	1
77.945	1282960	$2p^4\ {}^3P_2$	$-\ 4d\ {}^3D^o_{1,2,3}$	10	

TABLE X

STRONG EMISSION LINES OF Al VII

Wave Length	Wave Number	Term Combination	Intensity
356.885	280202	$2p^3\ {}^4S^o_{1\frac{1}{2}} - 2p^4\ {}^4P_{2\frac{1}{2}}$	5
353.776	282665	$2p^3\ {}^4S^o_{1\frac{1}{2}} - 2p^4\ {}^4P_{1\frac{1}{2}}$	9
352.160	283962	$2p^3\ {}^4S^o_{1\frac{1}{2}} - 2p^4\ {}^4P_{\frac{1}{2}}$	2
309.122	323497	$2p^3\ {}^2D^o_{2\frac{1}{2}} - 2p^4\ {}^2D_{2\frac{1}{2}}$	2
309.012	323612	$2p^3\ {}^2D^o_{1\frac{1}{2}} - 2p^4\ {}^2D_{1\frac{1}{2}}$	2
240.770	415334	$2p^3\ {}^2D^o_{2\frac{1}{2}} - 2p^4\ {}^2P_{1\frac{1}{2}}$	4
239.030	418358	$2p^3\ {}^2D^o_{1\frac{1}{2}} - 2p^4\ {}^2P_{\frac{1}{2}}$	2
88.033	1135940	$2p^3\ {}^2D^o_{2\frac{1}{2},1\frac{1}{2}} - 3s'\ {}^2D_{2\frac{1}{2},\ 1\frac{1}{2}}$	18
87.060	1148630	$2p^3\ {}^4S^o_{1\frac{1}{2}} - 3s\ \ {}^4P_{1\frac{1}{2}}$	12
86.887	1150920	$2p^3\ {}^4S^o_{1\frac{1}{2}} - 3s\ \ {}^4P_{2\frac{1}{2}}$	15
79.197	1262670	$2p^3\ {}^2D^o_{1\frac{1}{2}} - 3d\ \ {}^2F_{2\frac{1}{2}}$	10
79.012	1265630	$2p^3\ {}^2D^o_{2\frac{1}{2}} - 3d\ \ {}^2F_{3\frac{1}{2}}$	15
78.351	1276310	$2p^3\ {}^2P^o_{\frac{1}{2}} - 3d'\ {}^2D_{1\frac{1}{2}}$	20
78.327	1276700	$2p^3\ {}^2P^o_{1\frac{1}{2}} - 3d'\ {}^2D_{2\frac{1}{2}}$	20
77.945	1282960	$2p^3\ {}^2D^o_{1\frac{1}{2}} - 3d\ \ {}^2D_{1\frac{1}{2}}$	10
77.896	1283760	$2p^3\ {}^2D^o_{2\frac{1}{2}} - 3d\ \ {}^2D_{2\frac{1}{2}}$	10
76.572	1305960	$2p^3\ {}^2D^o_{2\frac{1}{2}} - 3d'\ {}^2F_{3\frac{1}{2}}$	20

TABLE X (Continued)

Wave Number	Wave Number	Term Combination	Intensity
76.543	1306460	$2p^3\ ^2D^o_{1\frac{1}{2}} - 3d'\ ^2F_{2\frac{1}{2}}$	20
76.422	1308520	$2p^3\ ^2D^o_{1\frac{1}{2}} - 3d'\ ^2D_{1\frac{1}{2}}$	10
76.383	1309190	$2p^3\ ^2D^o_{2\frac{1}{2}} - 3d'\ ^2D_{2\frac{1}{2}}$	10
75.360	1326960	$2p^3\ ^4S^o_{1\frac{1}{2}} - 3d\ ^4P_{2\frac{1}{2}}$	12
72.270	1383700	$2p^3\ ^4S^o_{1\frac{1}{2}} - 3p'''\ ^4P_{2\frac{1}{2}}$	10
63.025	1586670	$2p^3\ ^2D^o_{2\frac{1}{2}} - 4d'\ ^2F$	10

TABLE XI

STRONG EMISSION LINES OF Al VIII

Wave Length	Wave Number	Term Combination		Intensity
78.351	1276310	$2p^3\ ^3P$	$- 3s^1\ ^3D$	20
68.375	1462520	$2p^2\ ^1D_2$	$- 3d\ ^1F^o_3$	15
67.946	1471760	$2p^3\ ^3D^o_3$	$- 3d^1\ ^3F_{4,3,2}$	10
67.464	1482270	$2p^2\ ^3P_2$	$- 3d\ ^3D^o_3$	12
67.408	1483500	$2p^2\ ^3P_1$	$- 3d\ ^2D^o_2$	10
67.288	1486150	$2p^2\ ^3P_2$	$- 3d\ ^3P^o_2$	10

APPENDIX C

TABLES OF EXCITED ENERGY LEVELS OF ALUMINUM

The following tables list the excited energy levels of the Aluminum ions I through VIII. The information, except for Al I, is taken from the work by C. E. Moore (1949). The information for Al I is taken from a 1963 article by Erikson and Isberg.

Erikson and Isberg have made several improvements in the term designations for Al I. They are 3d' ^2F, 4d ^2F, and 5d' ^2D, replacing 5s' ^2P, 4d' ^2Pm 6s' ^2P, and 5d' ^2F, respectively. Also, the term 3d' ^2P was discarded with the identification of the level 5s' $^4P_{2\frac{1}{2}}$.

The values of the energy levels for Al I are also those of Erikson and Isberg.

TABLE XII

EXCITED ENERGY LEVELS OF Al I

Configuration	Designation	J	Level
$3s^2(^1S_o)3p$	$3p\ ^2P$	½	0
		1½	112.061
$3s^2(^1S_o)4s$	$4s\ ^2S$	½	25347.756
$3s\ 3p^2$	$3p^2\ ^4P$	½	29020.41
		1½	29066.96
		2½	29142.78
$3s^2(^1S_o)3d$	$3d\ ^2D$	1½	32435.435
		2½	32436.778
$3s^2(^1S_o)4p$	$4p\ ^2P$	½	32949.804
		1½	32965.643
$3s^2(^1S_o)5s$	$5s\ ^2S$	½	37689.413
$3s^2(^1S_o)4d$	$4d\ ^2D$	1½	38929.405
		2½	38933.961
$3s^2(^1S_o)5p$	$5p\ ^2P$	½	40277.965
		1½	40277.872
$3s^2(^1S_o)4f$	$4f\ ^2F$	2½	41319.372
		3½	41319.380
$3s^2(^1S_o)6s$	$6s\ ^2S$	½	42144.402
$3s^2(^1S_o)5d$	$5d\ ^2D$	1½	42233.722
		2½	42237.781
$3s^2(^1S_o)6p$	$6p\ ^2P$	½	43335.013
		1½	43337.877
$3s^2(^1S_o)5f$	$5f\ ^2F$	2½	43831.090
		3½	43831.094

TABLE XII (Continued)

Configuration	Designation	J	Level
$3s^2(^1S_o)6d$	6d ^2D	1½	44166.417
		2½	44168.863
$3s^2(^1S_o)7s$	7s ^2S	½	44273.122
$3s^2(^1S_o)7p$	7p ^2P	½	44919.654
		1½	44921.275
$3s^2(^1S_o)6f$	6f ^2F	2½,3½	45194.663
$3s^2(^1S_o)7d$	7d ^2D	1½	45344.164
		2½	45345.598
$3s^2(^1S_o)8s$	8s ^2S	½	45457.233
$3s^2(^1S_o)7f$	7f	2½,3½	46015.756
$3s^2(^1S_o)8d$	8d ^2D	1½	46093.424
		2½	46094.316
$3s^2(^1S_o)9s$	9s ^2S	½	46183.896
$3s^2(^1S_o)8f$	8f ^2F	2½,3½	46547.924
$3s^2(^1S_o)9d$	9d ^2D	1½	46593.32
		2½	46593.95
$3s^2(^1S_o)10d$	10d ^2D	1½	46940.97
		2½	46941.55
$3s^2(^1S_o)11d$	11d ^2D	2½	47192.30
Al II ('S)	Limit	-----	48278.37
$3s\ 3p^2$	$3p^2$ ^2S	½	51753.0
$3s\ sp^2$	$3p^2$ ^2P	½	56636.93
		1½	56724.98
$3s3p(^3P)4s$	4s' ^4P	½	61691.46
		1½	61747.56
		2½	61843.54

TABLE XII (Continued)

Configuration	Designation	J	Level
$3s3p(^3P)3d$	$3d'\ ^2D$	1½	67635.13
		2½	67662.96
$3s3p(^3P)3d$	$3d'\ ^4D$	½	71235.25
		1½	71244.17
		2½	71260.55
		3½	71286.4
$3s3p(^3P)3d$	$3d'\ ^2F$	2½	72978.9
		3½	73077.8
$3s3p(^3P)5s$	$5s'\ ^4P$	2½	74979.02
$3s3p(^3P)4d$	$4d'\ ^2D$	1½	76521.6
		2½	76553.46
$3s3p(^3P)4d$	$4d'\ ^2F$	2½	78612.23
		3½	78710.26
$3s3p(^3P)5d$	$5d'\ ^2D$	1½	80158.0
		2½	80191.9
Al II (^3P)	Limit	------	85671.32

TABLE XIII

EXCITED ENERGY LEVELS OF Al II

Configuration	Designation	J	Level
$3s^2$	$3s^2$ ^1S	0	0.0
$3s(^2S)3p$	3p $^3P^o$	0	37392.0
		1	37453.8
		2	37579.3
$3s(^2S)3p$	3p $^1P^o$	1	59849.7
$3p^2$	$3p^2$ ^1D	2	85479.0
$3s(^2S)4s$	4s ^3S	1	91271.2
$3p^2$	$3p^2$ ^3P	0	94084.5
		1	94146.8
		2	94267.7
$3s(^2S)4s$	4s ^1S	0	95348.2
$3s(^2S)3d$	3d ^3D	3	95546.8
		2	95547.9
		1	95548.8
$3s(^2S)4p$	4p $^3P^o$	0	105424.3
		1	105438.4
		2	105467.7
$3s(^2S)4p$	4p $^1P^o$	1	106918.2
$3s(^2S)3d$	3d ^1D	2	110087.5
$3s(^2S)5s$	5s ^3S	1	120089.8
$3s(^2S)5s$	5s ^1S	0	121365.2
$3s(^2S)4d$	4d ^3D	3	121480.3
		2	121480.9
		1	121481.2
$3s(^2S)4f$	4f $^3F^o$	2	123415.9
		3	123418.0
		4	123420.8

TABLE XIII(Continued)

Configuration	Designation		J	Level
$3s(^2S)4f$	4f	$^1F^o$	3	123468.1
$3s(^2S)4d$	4d	^1S	2	124792.0
$3s(^2S)5p$	5p	$^3P^o$	0	125700.5
			1	125706.2
			2	125719.0
$3s(^2S)5p$	5p	$^1P^o$	1	125866.7
$3s(^2S)6s$	6s	^3S	1	132213.2
$3s(^2S)6s$	6s	^1S	0	132776.4
$3s(^2S)5d$	5d	^3D	3	132819.7
			2,1	132819.9
$3s(^2S)5f$	5f	$^3F^o$	2	133435.0
			3	133440.4
			4	133447.3
$3s(^2S)5f$	5f	$^1F^o$	3	133679.3
$3s(^2S)5d$	5d	^1D	2	133914.1
$3s(^2S)5g$	5g	^3G	3,2,5	134181.2
$3s(^2S)5g$	5g	^1G	4	134181.2
$3s(^2S)6p$	6p	$^1P^o$	1	134917.3
$3s(^2S)6p$	6p	$^3P^o$	0	135009.0
			1	135012.1
			2	135018.9
$3s(^2S)7s$	7s	^3S	1	138496.7
$3s(^2S)6f$	6f	$^3F^o$	2	138518.7
			3	138536.4
			4	138559.2
$3s(^2S)7s$	7s	^1S	0	138799.3
$3s(^2S)6d$	6d	^3D	3,2,1	138811.9

TABLE XIII (Continued)

Configuration	Designation		J	Level
$3s(^2S)6f$	6f	$^1F^o$	3	139242.9
$3s(^2S)6d$	6d	^1D	2	139286.8
$3s(^2S)6g$	6g	^3G	3,4,5	139588.7
$3s(^2S)6g$	6g	^1G	4	139558.7
$3s(^2S)7p$	7p	$^1P^o$	1	139916.7
$3s(^2S)7p$	7p	$^3P^o$	0,1,2	140091.2
$3p(^2P^o)3d$	3d	$^3F^o$	2	141082.4
			3	141107.5
			4	141140.5
$3s(^2S)8s$	8s	^3S	1	142179.8
$3s(^2S)8s$	8s	^1S	0	142360.8
$3s(^2S)7d$	7d	^3D	3,2,1	142362.8
$3s(^2S)7f$	7f	$^1F^o$	3	142601.6
$3s(^2S)7d$	7d	^1D	2	142607.0
$3s(^2S)7g$	7g	^3G	3,4,5	142849.2
$3s(^2S)7g$	7g	^1G	4	142849.2
$3s(^2S)8p$	8p	$^1P^o$	1	142958.9
$3s(^2S)8p$	8p	$^3P^o$	0,1,2	143180.0
$3s(^2S)7f$	7f	$^3F^o$	2	143262.7
			3	143269.8
			4	143280.6
$3s(^2S)9s$	9s	^2S	1	144524.3
$3s(^2S)8d$	8d	^3D	3,2,1	144638.9
$3s(^2S)9s$	9s	^1S	0	144641.9

TABLE XIII (Continued)

Configuration	Designation	J	Level
$3s(^2S)8d$	8d ^1D	2	144780.2
$3s(^2S)8f$	8f $^1F^o$	3	144781.9
$3s(^2S)9p$	9p $^1P^o$	1	144939.1
$3s(^2S)8g$	8g ^3G	3,4,5	144964.7
$3s(^2S)8g$	8g ^1G	4	144964.7
$3s(^2S)8g$	8h $^3H^o$	4,5,6	144990.0
$3s(^2S)8h$	8h $^1H^o$	5	144990.0
$3s(^2S)8f$	8f $^3F^o$	2	145126.5
		3	145128.9
		4	145132.1
$3p(^2P^o)3d$	3d $^3D^o$	1,2	145148
		3	145152
$3s(^2S)9p$	9p $^3P^o$	0.1.2	145185
$3p(^2P^o)4s$	4s $^3P^o$	0	145773.9
		1	145832.6
		2	145959.4
$3s(^2S)10s$	10s ^3S	1	146108.8
$3s(^2S)9d$	9d ^3D	3,2,1	146185.0
$3s(^2S)10s$	10s ^1S	0	146190.1
$3s(^2S)9d$	9d ^1D	2	146274.4
$3s(^2S)9f$	9f $^1F^o$	3	146276.5
$3s(^2S)10p$	10p $^1P^o$	1	146297.5
$3s(^2S)9g$	9g ^3G	3,4,5	146414.5
$3s(^2S)9g$	9g ^1G	4	146414.5

TABLE XIII (Continued)

Configuration	Designation	J	Level
$3s(^2S)9h$	9h $^3H^o$	4,5,6	146
$3s(^2S)9h$	9h $^1H^o$	5	146432.8
$3s(^2S)9f$	9f $^3F^o$	2	146496.7
		3	146497.8
		4	146499.2
$3s(^2S)10p$	10p $^3P^o$	0,1,2	146577
$3p(^2P^o)3d$	3d $^3P^o$	0	146595.0
		1	146596.9
		2	146599.3
$3s(^2S)11s$	11s ^3S	1	147229.0
$3s(^2S)11p$	11p $^1P^o$	1	147268.8
$3s(^2S)10d$	10d ^3D	3,2,1	147282.8
$3s(^2S)11s$	11s ^1S	0	147288.8
$3s(^2S)10d$	10d ^1D	2	147343.2
$2s(^2S)10f$	10f $^1F^o$	3	147344.2
$3s(^2S)10g$	10g ^3G	3,4,5	147451.0
$3s(^2S)10g$	10g ^3G	3,4,5	147451.0
$3s(^2S)10h$	10h $^3H^o$	3,4,5	147464.7
$3s(^2S)10h$	10h $^1H^o$	5	147464.7
$3s(^2S)10f$	10f $^3F^o$	2	147499.8
		3	147500.2
		4	147500.8
$3s(^2S)11p$	11p $^2P^o$	0,1,2	147572
$3p(^2P^o)4s$	4s $^1P^o$	1	148002.0
$3s(^2S)12s$	12s ^3S	1	148052.5

TABLE XIII (Continued)

Configuration	Designation	J	Level
$3s(^2S)11d$	$11d\ ^3D$	3,2,1	148090.0
$3s(^2S)12s$	$12s\ ^1S$	0	148097.1
$3s(^2S)11f$	$11f\ ^1F^o$	3	148132.6
$3s(^2S)11d$	$11d\ ^1D$	2	148132.7
$3s(^2S)11g$	$11g\ ^3G$	3,4,5	148217.6
$3s(^2S)11g$	$11g\ ^1G$	4	148217.6
$3s(^2S)11f$	$11f\ ^3F^o$	2	148248.7
		3	148249.1
		4	148249.6
$3s(^2S)12p$	$12p\ ^1P^o$	1	148579.4
$3s(^2S)13s$	$13s\ ^3S$	1	148673.7
$3s(^2S)13s$	$13s\ ^1S$	0	148706.9
$3s(^2S)12f$	$12f\ ^1F^o$	3	148731.6
$3s(^2S)12g$	$12g\ ^3G$	3,4,5	148800.4
$3s(^2S)12g$	$12g\ ^1G$	4	148800.4
$3s(^2S)12f$	$12f\ ^3F^o$	2,3,4	148822.5
$3s(^2S)13p$	$13p\ ^1P^o$	1	149051.9
$3s(^2S)14s$	$14s\ ^1S$	0	149179.8
$3s(^2S)13f$	$13f\ ^1F^o$	3	149199.2
$3s(^2S)13g$	$13g\ ^3G$	3,4,5	149252.9
$3s(^2S)13g$	$13g\ ^1G$	4	149252.9
$3s(^2S)13f$	$13f\ ^3F^o$	2,3,4	149269.5
$3s(^2S)14p$	$14p\ ^1P^o$	1	149434.8

TABLE XIII (Continued)

Configuration	Designation	J	Level
3s(^{2}S)15s	15s ^{1}S	0	149554.7
3s(^{2}S)14f	14f ^{1}F^o	3	149568.6
3s(^{2}S)14f	14f ^{3}F^o	2,3,4	149625.5
3s(^{2}S)15p	15p ^{1}P^o	1	149748.0
3s(^{2}S)16s	16s ^{1}S	0	149856.6
3s(^{2}S)15f	15f ^{1}F^o	3	149866.2
3s(^{2}S)15f	15f ^{3}F^o	2,3,4	149913.2
3s(^{2}S)16p	16p ^{1}P^o	1	150007.6
3s(^{2}S)16f	16f ^{1}F^o	3	150109.7
3s(^{2}S)16f	16f ^{3}F^o	2,3,4	150109.7
3s(^{2}S)17f	17f ^{3}F^o	3	150311.1
3s(^{2}S)17f	17f ^{3}F^o	2,3,4	150343.5
3s(^{2}S)18f	18f ^{1}F^o	3	150479.7
3s(^{2}S)19f	19f ^{1}F^o	3	150622.2
3s(^{2}S)20f	20f ^{1}F^o	3	150744.1
Al III (^{2}S$_{1/2}$)	Limit	-----	151860.4

TABLE XIV

EXCITED ENERGY LEVELS OF Al III

Configuration	Designation	J	Level
3s	3s ^2S	½	0.00
3p	3p $^2P^o$	½	53684.1
		1½	53916.6
3d	3d ^2D	2½	115955.03
		1½	115957.31
4s	4s ^2S	½	126162.58
4p	4p $^2P^o$	½	143632.25
		1½	143712.38
4d	4d ^2D	2½	165785.26
		1½	165786.54
4f	4f $^2F^o$	2½	167612.05
		3½	167612.43
5s	5s ^2S	½	170636.38
5p	5p $^2P^o$	½	178430.49
			178469.64
5d	5d ^2D	{2½, 1½}	188875.52
5f	5f $^2F^o$	2½	189875.34
		3½	189875.46
5g	5g ^2G	{3½, 4½}	189927.76
6s	6s ^2S	½	191478.5

TABLE XIV (Continued)

Configuration	Designation	J	Level
6p	6p $^2P^o$	½ 1½	195620.94 195641.53
6d	6d ^2D	{2½, 1½}	201374.37
6f	6f $^2F^o$	{2½, 3½}	201969.52
6g	6g ^2G	{3½, 4½}	202001.32
6h	6h $^2H^o$	{4½, 5½}	202007.32
7s	7s ^2S	½	202904.8
7p	7p $^2P^o$	{½, 1½}	205360
7d	7d ^2D	{2½, 1½}	208880.37
7f	7f $^2F^o$	{2½, 3½}	209260.98
7g	7g ^2G	{3½, 4½}	209282.17
7h	7h $^2H^o$	{4½, 5½}	209287.52
8d	8d ^2D	{2½, 1½}	213741.42
8f	8f $^2F^o$	{2½, 3½}	213992.12
8g	8g ^2G	{3½, 4½}	214010.67
8h	8h $^2H^o$	{4½, 5½}	214015.8

TABLE XIV (Continued)

Configuration	Designation	J	Level
9h	9h $^2H^o$	{4½, 5½}	217255.2
Al IV (^1S)	Limit	------	229453.99

TABLE XV

EXCITED ENERGY LEVELS OF Al IV

Configuration	Designation	J	Level
$2p^6$	$2p^6\ ^1S$	0	0
$2p^5(^2P^o_{1\frac{1}{2}})3s$	$3s\ [1\frac{1}{2}]^o$	2	616646.7
		1	628477.5
$2p^5(^2P^o_{\frac{1}{2}})3s$	$3s'\ [\frac{1}{2}]^o$	0	619947.7
		1	624720.5
$2p^5(^2P^o_{1\frac{1}{2}})3p$	$3p\ [\frac{1}{2}]$	1	671635.5
"	$3p\ [2\frac{1}{2}]$	3	680862.9
		2	681686.7
"	$3p\ [1\frac{1}{2}]$	1	682869.3
		2	685732.8
"	$3p\ [\frac{1}{2}]$	0	688313.3
$2p^5(^2P^o_{\frac{1}{2}})3p$	$3p'\ [1\frac{1}{2}]$	1	687456.8
		2	687834.7
"	$3p'\ [\frac{1}{2}]$	1	688653.0
		0	690244.9
$2p^5(^2P^o_{1\frac{1}{2}})3d$	$3d\ [\frac{1}{2}]^o$	0	759197.4
		1	759600.9
"	$3d\ [1\frac{1}{2}]^o$	2	761015.4
"	$3d\ [3\frac{1}{2}]^o$	4	761694.5
		3	762277.1
"	$3d\ [2\frac{1}{2}]^o$	2	763502.8
		3	764304.3
"	$3d\ [1\frac{1}{2}]^o$	1	767040.6

TABLE XV (Continued)

Configuration	Designation	J	Level
$2p^5(^2P^o_{\frac{1}{2}})3d$	$3d'[2\frac{1}{2}]^o$	3	767351.9
		2	767536.2
"	$3d'[1\frac{1}{2}]^o$	2	767756.1
		1	770836.1
$2p^5(^2P^o_{1\frac{1}{2}})4s$	$4s\ [1\frac{1}{2}]^o$	2	
		1	802936
$2p^5(^2P^o_{\frac{1}{2}})4s$	$4s'\ [\frac{1}{2}]^o$	0	
		1	806231
$2p^5(^2P^o_{1\frac{1}{2}})4d$	$4d\ [\frac{1}{2}]^o$	0	
		1	851950
"	$4d\ [1\frac{1}{2}]^o$	1	855286
$2p^5(^2P^o_{\frac{1}{2}})4d$	$4d'\ [1\frac{1}{2}]^o$	2	
		1	858671
$2p^5(^2P^o_{1\frac{1}{2}})5s$	$5s\ [1\frac{1}{2}]^o$	2	
		1	871391
$2p^5(^2P^o_{\frac{1}{2}})5s$	$5s'\ [\frac{1}{2}]^o$	0	
		1	874669
$2p^5(^2P^o_{1\frac{1}{2}})5d$	$5d\ [\frac{1}{2}]^o$	0	
		1	894614
"	$5d\ [1\frac{1}{2}]^o$	1	896138
$2p^5(^2P^o_{\frac{1}{2}})5d$	$5d'\ [1\frac{1}{2}]^o$	2	
		1	899281
$2p^5(^2P^o_{1\frac{1}{2}})6d$	$6d\ [1\frac{1}{2}]^o$	1	918215
$2p^5(^2P^o_{\frac{1}{2}})6d$	$6d'\ [1\frac{1}{2}]^o$	2	
		1	921362
Al V $(^2P^o_{1\frac{1}{2}})$	Limit	-----	967783
Al V $(^2P^o_{\frac{1}{2}})$	Limit	-----	971223

TABLE XVI

EXCITED ENERGY LEVELS OF Al V

Configuration	Designation	J	Level
$2s^2\ 2p^5$	$2p^5\ ^2P^o$	1½	0
		½	3440
$2s\ 2p^6$	$2p^6\ ^2S$	½	358810
$2s^2\ 2p^4(^3P)3s$	$3s\ ^4P$	2½	751810
		1½	753960
		½	755250
$2s^2\ 2p^4(^3P)3s$	$3s\ ^2P$	1½	764240
		½	766790
$2s^2\ 2p^4(^1D)3s$	$3s'\ ^2D$	2½	796650
		1½	796680
$2s^2\ 2p^4(^1S)3s$	$3s''\ ^2S$	½	843880
$2s^2\ 2p^4(^3P)3d$	$3d\ ^4D$	3½	
		2½	919900
		1½	920680
		½	
$2s^2\ 2p^4(^3P)3d$	$3d\ ^4P$	½	921440
		1½	922120
		2½	922640
$2s^2\ 2p^4(^3P)3d$	3d 2F	3½	
		2½	923230
$2s^2\ 2p^4(^3P)3d$	$3d\ ^2D$	1½	925430
		2½	926400
$2s^2\ 2p^4(^3P)3d$	$3d\ ^2P$	½	925900
		1½	928410

TABLE XVI (Continued)

Configuration	Designation	J	Level
$2s^2\ 2p^4(^1D)3d$	$3d'\ ^2P$	½	960420
		1½	961630
$2s^2\ 2p^4(^1D)3d$	$3d'\ ^2S$	½	960860
$2s^2\ 2p^4(^1D)3d$	$3d'\ ^2D$	2½	962640
		1½	963330
$2s^2\ 2p^4(^3P)4s$	$4s\ ^2P$	1½	1005760
		½	1008040
$2s^2\ 2p^4(^1S)3d$	$3d''\ ^2D$	2½	1007150
		1½	1007290
$2s^2\ 2p^4(^1D)4s$	$4s'\ ^2D$	2½	1043430
		1½	1043480
$2s^2\ 2p^4(^3P)4d$	$4d\ ^4D$	3½	
		2½	1062510
		1½	1062820
		½	
$2s^2\ 2p^4(^3P)4d$	$4d\ ^4P$	½	
		1½	1063650
		2½	1064050
$2s^2\ 2p^4(^3P)4d$	$4d\ ^2P$	½	1065170
		1½	1067770
$2s^2\ 2p^4(^3P)4d$	$4d\ ^2D$	1½	1065460
		2½	1066610
$2s^2\ 2p^4(^1S)4s$	$4s''\ ^2S$	½	1089930
$2s\ 2p^5(^3P^o)3s$	$3s'''\ ^2P^o$	1½	1096180
		½	1098350
$2s^2\ 2p^4(^1D)4d$	$4d'\ ^2P$	½	1101400
		1½	1103380
$2s^2\ 2p^4(^1D)4d$	$4d'\ ^2S$	½	1102540
$2s^2\ 2p^4(^1D)4d$	$4d'\ ^2D$	2½	1103190
		1½	

TABLE XVI (Continued)

Configuration	Designation	J	Level
$2s^2\ 2p^4(^3P)5d$	5d ^4D	3½	
		2½	1127550
		1½	1127730
		½	
$2s^2\ 2p^4(^3P)5d$	5d ^2D	1½	1129350
		2½	1130900
$2s^2\ 2p^4(^3P)5d$	5d ^2P	½	1129350
		1½	1131650
$2s^2\ 2p^4(^1S)4d$	4d" ^2D	2½	1149160
		1½	1149260
$2s^2\ 2p^4(^3P)6d$	6d ^2D	1½	1163850
		2½	1165450
$2s^2\ 2p^4(^1D)5d$	5d' ^2S	½	1167380
$2s^2\ 2p^4(^1D)5d$	5d' ^2P	½	
		1½	1168060
Al VI ($^3P_2$)	Limit	-----	1240600

TABLE XVII

EXCITED ENERGY LEVELS OF Al VI

Configuration	Designation	J	Level
$2s^2\ 2p^4$	$2p^4\ ^3P$	2	0
		1	2736
		0	3831
$2s^2\ 2p^4$	$2p^4\ ^1D$	2	41600
$2s^2\ 2p^4$	$2p^4\ ^1S$	0	88670
$2s\ \ 2p^5$	$2p^5\ ^3P^o$	2	323002
		1	325470
		0	326622
$2s\ \ 2p^5$	$2p^5\ ^1P^o$	1	451840
$2s^2\ 2p^3(^4S^o)3s$	$3s\ \ ^3S^o$	1	913130
$2s^2\ 2p^3(^2D^o)3s$	$3s'\ ^3D^o$	3,2,1	961100
$2s^2\ 2p^3(^2D^o)3s$	$3s'\ ^1D^o$	2	970790
$2s^2\ 2p^3(^2P^o)3s$	$3s''\ ^3P^o$	0	
		1	993660
		2	993880
$2s^2\ 2p^3(^2P^o)3s$	$3s''\ ^1P^o$	1	1003700
$2s^2\ 2p^3(^4S^o)3d$	$3d\ \ ^3D^o$	1	1079460
		2	1079490
		3	1079610
$2s^2\ 2p^3(^2D^o)3d$	$3d'\ ^3F^o$	4	
		3	
		2	1132180
$2s^2\ 2p^3(^2D^o)3d$	$3d'\ ^3D^o$	3,2,1	1134170

TABLE XVII (Continued)

Configuration	Designation	J	Level
$2a^2\ 2p^3(^2D^o)3d$	$3d'\ ^1P^o$	1	1136500
$2s^2\ 2p^3(^2D^o)3d$	$3d'\ ^3P^o$	2	1140840
		1	1141670
		0	1141910
$2s^2\ 2p^3(^2D^o)3d$	$3d'\ ^1D^o$	2	1142220
$2s^2\ 2p^3(^2D^o)3d$	$3d'\ ^3S^o$	1	1145020
$2s^2\ 2p^3(^2D^o)3d$	$3d'\ ^1F^o$	3	1150250
$2s^2\ 2p^3(^2P^o)3d$	$3d''\ ^3P^o$	0	1164220
		1	1164620
		2	1165260
$2s^2\ 2p^3(^2P^o)3d$	$3d''\ ^3F^o$	4	
		3	1166530
		2	1168690
$2s^2\ 2p^3(^2P^o)3d$	$3d''\ ^1D^o$	2	1169150
$2s^2\ 2p^3(^2P^o)3d$	$3d''\ ^3D^o$	3	1169390
		2	1170650
		1	
$2s^2\ 2p^3(^2P^o)3d$	$3d''\ ^1P^o$	1	1171050
$2s^2\ 2p^3(^2P^o)3d$	$3d''\ ^1F^o$	3	1174450
$2s\ \ 2p^4(^4P)3s$	$3s'''\ ^3P$	2	1204550
		1	1205500
		0	
$2s^2\ 2p^3(^4S^o)4s$	$4s\ \ ^3S^o$	1	1218290
$2s^2\ 2p^3(^2D^o)4s$	$4s'\ ^3D^o$	3,2,1	1274550
$2s^2\ 2p^3(^2D^o)4s$	$4s'\ ^1D^o$	2	1279680
$2s^2\ 2p^3(^4S^o)4d$	$4d\ \ ^3D^o$	1,2,3	1282960
$2s\ \ 2p^4(^2D)3s$	$3s^{IV}\ ^3D$	3,2,1	1293290

TABLE XVII (Continued)

Configuration	Designation	J	Level
$2s^2\ 2p^3(^2P^o)4s$	$4s'\ ^1P^o$	1	1312070
$2s^2\ 2p^3(^2D^o)4d$	$4d'\ ^3D^o$	3,2,1	1339480
$2s^2\ 2p^3(^2D^o)4d$	$4d'\ ^1P^o$	1	1341090
$2s^2\ 2p^3(^2D^o)4d$	$4d'\ ^3P^o$	2	1343320
		1	
		0	
$2s^2\ 2p^3(^2D^o)4d$	$4d'\ ^3S^o$	1	1345030
$2s^2\ 2p^3(^2D^o)4d$	$4d'\ ^1D^o$	2	1345430
$2s^2\ 2p^3(^2D^o)4d$	$4d'\ ^1F^o$	3	1346780
$2s\ \ 2p^4(^2S)3s$	$3s^V\ ^3S$	1	1359890
$2s^2\ 2p^3(^2P^o)4d$	$4d''\ ^3P^o$	0	
		1	
		2	1371220
$2s^2\ 2p^3(^2P^o)4d$	$4d''\ ^3D^o$	3	1373440
		2	1375140
		1	
$2s^2\ 2p^3(^4S^o)5d$	$5d\ \ ^3D^o$	1,2,3	1375250
$2s^2\ 2p^3(^2P^o)4d$	$4d''\ ^1F^o$	3	1376860
$2s^2\ 2p^3(^2D^o)5s$	$5s'\ ^1D^o$	2	1405220
$2s^2\ 2p^3(^2P^o)5d$	$5d''\ ^3P^o$	0	
		1	
		2	1465780
$2s^2\ 2p^3(^2P^o)5d$	$5d''\ ^3D^o$	3	1466990
		2	
		1	
Al VII ($^4S^o_{1\frac{1}{2}}$)	Limit	------	1536300

TABLE XVIII

EXCITED ENERGY LEVELS OF Al VII

Configuration	Designation	J	Level
$2s^2\ 2p^3$	$2p^3\ {}^4S^o$	1½	0
$2s^2\ 2p^3$	$2p^3\ {}^2D^o$	1½	60700
		2½	60760
$2s^2\ 2p^3$	$2p^3\ {}^2P^o$	½	93000
		1½	93270
$2s\ \ 2p^4$	$2p^4\ {}^4P$	2½	280200
		1½	232660
		½	283960
$2s\ \ 2p^4$	$2p^4\ {}^2D$	2½	384260
		1½	384410
$2s\ \ 2p^4$	$2p^4\ {}^2S$	½	451360
$2s\ \ 2p^4$	$2p^4\ {}^2P$	1½	476090
		½	479050
$2s^2\ 2p^2({}^1S)3d$	$3d''\ {}^2D$	{1½, 2½}	1410380
$2s\ \ 2p^3({}^5S^o)3d$	$3d'''\ {}^4D^o$	{½ to 3½}	1473060
$2s^2\ 2p^2({}^3P)4s$	$4s\ \ {}^4P$	½	
		1½	1540740
		2½	1542850
$2s^2\ 2p^2({}^3P)4s$	$4s\ \ {}^2P$	½	
		1½	1540820
$2s\ \ 2p^3({}^3D^o)3d$	$3d^{IV}\ {}^4P^o$	2½	1591560
		1½	1592170
		½	1592550

TABLE XVIII (Continued)

Configuration	Designation	J	Level
$2s\ 2p^3(^3D^o)3d$	$3d^{IV}\ ^4D^o$	$\frac{1}{2}$ to $3\frac{1}{2}$	1598270
$2s^2\ 2p^2(^3P)4d$	$4d\ ^2P$	$1\frac{1}{2}$	1598890
		$\frac{1}{2}$	
$2s\ 2p^3(^3D^o)3d$	$3d^{IV}\ ^4S^o$	$1\frac{1}{2}$	1599300
$2s^2\ 2p^2(^3P)4d$	$4d\ ^4D$	$3\frac{1}{2}$	
		$2\frac{1}{2}$, $1\frac{1}{2}$	1600670
		$\frac{1}{2}$	1601740
$2s^2\ 2p^2(^3P)4d$	$4d\ ^2F$	$2\frac{1}{2}$	1603550
		$3\frac{1}{2}$	1606260
$2s^2\ 2p2(^3P)4d$	$4d\ ^4P$	$2\frac{1}{2}$	1605240
		$1\frac{1}{2}$	
		$\frac{1}{2}$	
$2s^2\ 2p^2(^3P)4d$	$4d\ ^2D$	$1\frac{1}{2}$	1610820
		$2\frac{1}{2}$	1611560
$2s^2\ 2p^2(^1D)4d$	$4d'\ ^2D$	$1\frac{1}{2}$	1646820
		$2\frac{1}{2}$	1647880
$2s^2\ 2p^2(^1D)4d$	$4d'\ ^2F$	$2\frac{1}{2}$, $3\frac{1}{2}$	1647430
$2s^2\ 2p^2(3P)3s$	$3s\ ^4P$	$\frac{1}{2}$	1147100
		$1\frac{1}{2}$	1148630
		$2\frac{1}{2}$	1150920
$2s^2\ 2p^2(^3P)3s$	$3s\ ^2P$	$\frac{1}{2}$	1162360
		$1\frac{1}{2}$	1165130
$2s^2\ 2p^2(^1D)3s$	$3s'\ ^2D$	$1\frac{1}{2}$, $2\frac{1}{2}$	1196680
$2s^2\ 2p^2(^1S)3s$	$3s''\ ^2S$	$\frac{1}{2}$	1246840
$2s^2\ 2p^2(^3P)3d$	$3d\ ^2P$	$1\frac{1}{2}$	1315640
		$\frac{1}{2}$	1316420

TABLE XVIII (Continued)

Configuration	Designation	J	Level
$2s\ 2p^3(^5S^o)3s$	$3s'''\ ^4S^o$	1½	1322180
$2s^2\ 2p^2(^3P)3d$	$3d\ ^2F$	2½	1323370
		3½	1326390
$2s^2\ 2p^2(^3P)3d$	$3d\ ^4D$	3½	
		{2½, 1½}	1323940
		½	1324710
$2s^2\ 2p^2(^3P)3d$	$3s\ ^4P$	2½	1326960
		1½	1327990
		½	1328550
$2s^2\ 2p^2(^3P)3d$	$3d\ ^2D$	1½	1343710
		2½	1344530
$2s^2\ 2p^2(^1D)3d$	$3d'\ ^2F$	3½	1366720
		2½	1367160
$2s^2\ 2p^2(^1D)3d$	$3d'\ ^2D$	1½	1369270
		2½	1369960
$2s^2\ 2p^2(^1D)3d$	$3d'\ ^2P$	½	1378290
		1½	1379130
$2s\ 2p^3(^5S^o)3p$	$3p'''\ ^4P$	{½ to 2½}	1383700
$2s^2\ 2p^2(^1D)3d$	$3d'\ ^2S$	½	1384370
$2s^2\ 2p^2(^1D)4d$	$4d'\ ^2S$	½	1654160
$2s^2\ 2p^2(^3P)5s$	$5s\ ^4P$	½	
		1½	
		2½	1702070
$2s^2\ 2p^2(^3P)5d$	$5d\ ^2F$	2½	1729840
		3½	1732410
$2s\ 2\frac{1}{2}^3(^5S^o)4d$	$4d'''\ ^4D^o$	3½	1739390
		2½	1739600
		{1½, ½}	1739970

TABLE XVIII (Continued)

Configuration	Designation	J	Level
$2s^2\ 2p^2(^1D)5d$	$5d'\ ^2F$	$\left\{\begin{matrix}3\frac{1}{2}\\2\frac{1}{2}\end{matrix}\right\}$	1773560
Al VIII (^3P_o)	Limit	-----	1951830

TABLE XIX

EXCITED ENERGY LEVELS OF Al VIII

Configuration	Designation	J	Level
$2s^2\ 2p^2$	$2p^2\ {}^3P$	0	0
		1	1740
		2	4440
$2s^2\ 2p^2$	$2p^2\ {}^1D$	2	46690
$2s^2\ 2p^2$	$2p^2\ {}^1S$	0	96170
$2s\ \ 2p^3$	$2p^3\ {}^5S^o$	2	133510
$2s\ \ 2p^3$	$2p^3\ {}^3D^o$	3	262190
		2	262320
		1	262390
$2s\ \ 2p^3$	$2p^3\ {}^3P^o$	0,1,2	309130
$2s\ \ 2p^3$	$2p^3\ {}^1D^o$	2	396990
$2s\ \ 2p^3$	$2p^3\ {}^3S^o$	1	404220
$2s\ \ 2p^3$	$2p^3\ {}^1P^o$	1	444550
$2s^2\ 2p(^2P^o)3s$	$3s\ \ {}^3P^o$	0	1319280
		1	1320450
		2	1324080
$2s^2\ 2p(^2P^o)3s$	$3s\ \ {}^1P^o$	1	1335270
$2s^2\ 2p(^2P^o)3p$	$3p\ \ {}^3S$	1	1402180
$2s\ \ 2p^2(^4P)3s$	$3s\ \ {}^5P$	1	1465810
		2	1467470
		3	1469680

TABLE XIX (Continued)

Configuration	Designation	J	Level
$2s^2\ 2p(^2P^o)3d$	3d $^3F^o$	2	1468700
		3	
		4	
$2s^2\ 2p(^2P^o)3d$	3d $^1D^o$	2	1471980
$2s^2\ 2p(^2P^o)3d$	3d $^3D^o$	1	1484560
		2	1485240
		3	1486710
$2s^2\ 2p(^2P^o)3d$	3d $^3P^o$	2	1490590
		1	1491570
		0	1492140
$2s\ \ 2p^2(^4P)3s$	3s ^3P	0	
		1	1504810
		2	1507220
$2s^2\ 2p(^2P^o)3d$	3d $^1F^o$	3	1509210
$2s^2\ 2p(^2P^o)3d$	3d $^1P^o$	1	1510060
$2s\ \ 2p^2(^4P)3p$	3p $^3S^o$	1	1531270
$2s\ \ 2p^2(^4P)3p$	3p $^3D^o$	1	1564140
		2	1564840
		3	1566840
$2s\ \ 2p^2(^4P)3p$	3p $^3P^o$	0	
		1	
		2	1577760
$2s\ \ 2p^2(^2D)3s$	3s' ^3D	1,2,3	1585400
$2s\ \ 2p^2(^2D)3s$	3s' ^1D	2	1608440
$2s\ \ 2p^2(^4P)3d$	3d ^5P	3	1631170
		2	1632060
		1	1632670
$2s\ \ 2p^2(^4P)3d$	3d ^3P	2	1633840
		1	1635440
		0	

TABLE XIX (Continued)

Configuration	Designation	J	Level
$2s\ 2p^2(^4P)3d$	$3d\ ^3F$	2	1643590
		3	1644990
		4	1646790
$2s\ 2p^2(^2D)3p$	$3p'\ ^1F^o$	3	1659180
$2s\ 2p^2(^2S)3s$	$3s''\ ^3S$	1	1662740
2s 2½^2(^{4}P)3d	$3d\ ^3D$	1	1664880
		2	1665380
		3	1665930
$2s\ 2p^2(^2D)3p$	$3p'\ ^1D^o$	2	1667490
$2s\ 2p^2(^2P)3s$	$3s'''\ ^3P$	0	
		1	
		2	1682590
$2s\ 2p^2(^2D)3d$	$3d'\ ^3F$	2,3,4	1733950
$2s\ 2p^2(^2D)3d$	$3d'\ ^3D$	1,2,3	1742250
$2s\ 2p^2(^2D)3d$	$3d'\ ^3P$	2	1745690
		1	1747940
		0	1749640
$2s\ 2p^2(^2D)3d$	$3d'\ ^3S$	1	1762090
$2s^2\ 2p(^2P^o)4s$	$4s\ ^3P^o$	0	
		1	
		2	1785380
2s 2o^2(^{2}S)3d	$3d''\ ^3D$	1	
		2	1815990
		3	1816950
$2s\ 2p^2(^2P)3d$	$3d'''\ ^3F$	2,3,4	1831700
$2s\ 2p^2(^2P)3d$	$3s'''\ ^3D$	1,2,3	1840570
$2s\ 2p^2(^2P)3d$	$3d'''\ ^3P$	0	
		1	
		2	1844390

TABLE XIX (Continued)

Configuration	Designation	J	Level
$2s^2\ 2p(^2P^o)4d$	4d $^3D^o$	1	
		2	1846180
		3	1847490
$2s^2\ 2p(^2P^o)4d$	4d $^1P^o$	1	1853670
$2s\ \ 2p^2(^4P)4d$	4d ^5P	3	1991450
		2	1992250
		1	1992760
$2s\ \ 2p^2(^4P)4d$	4d ^3F	2	
		3	1997710
		4	1999710
Al IX $(^2P^o_{1/2})$	Limit	--------	2300390

APPENDIX D

ENERGY LEVEL DIAGRAMS

The following diagrams for the Aluminum ions Al I through Al VIII show the relative positions of the excitation levels. The diagrams are approximately to scale, as indicated on each.

The information is taken from a 1949 work by C. E. Moore, except for Al I. The information for the Al I ion was taken from a 1963 article by Erikson and Isberg. Except for Al II all levels listed in Appendix C are shown. Only levels up to N=9 are shown for Al II. The remaining levels are too close together and too numerous to include without the diagram becoming excessively messy.

No attempt has been made to show the splitting of the levels over the quantum number J.

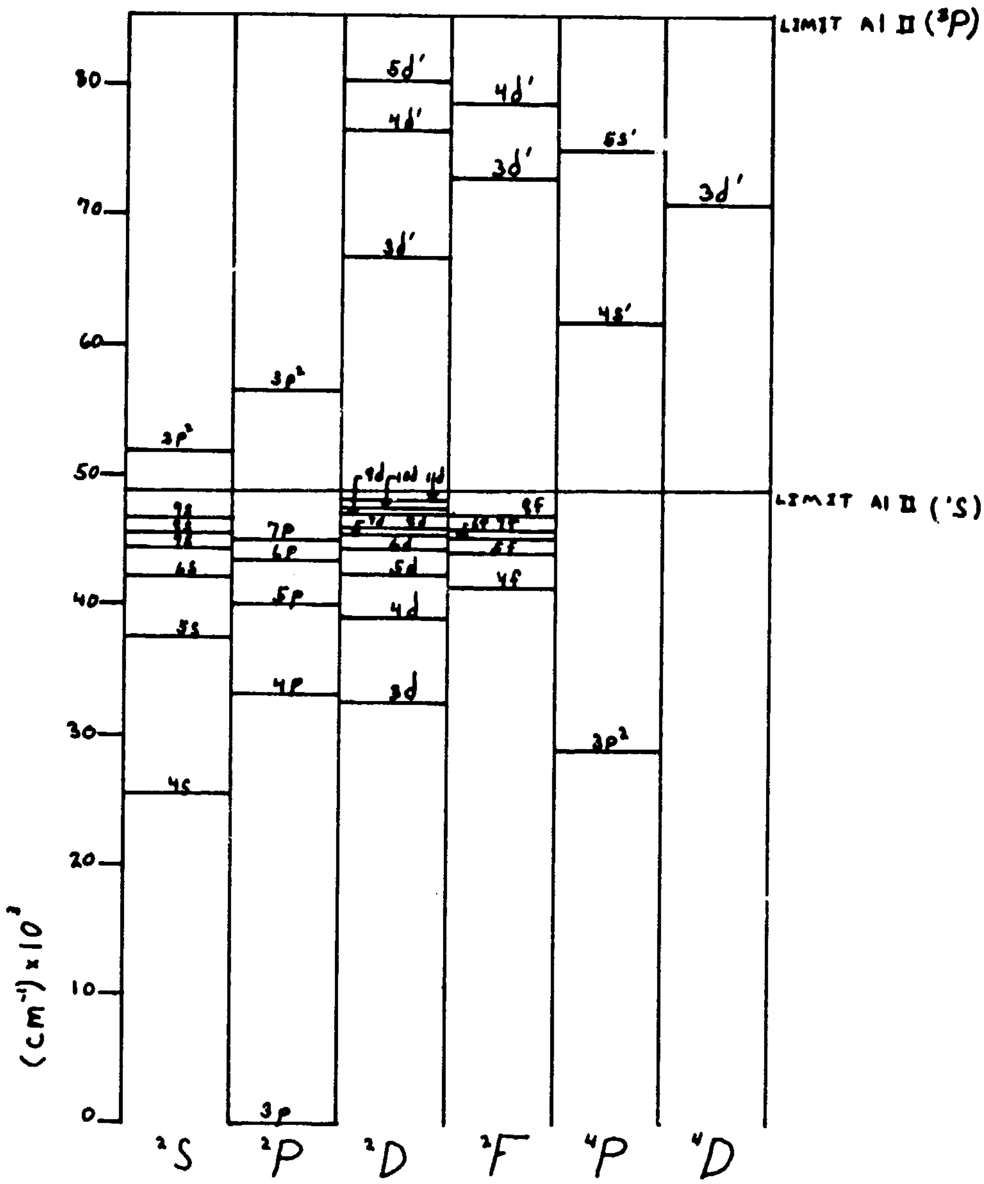

Figure 7. Energy Levels of Al I

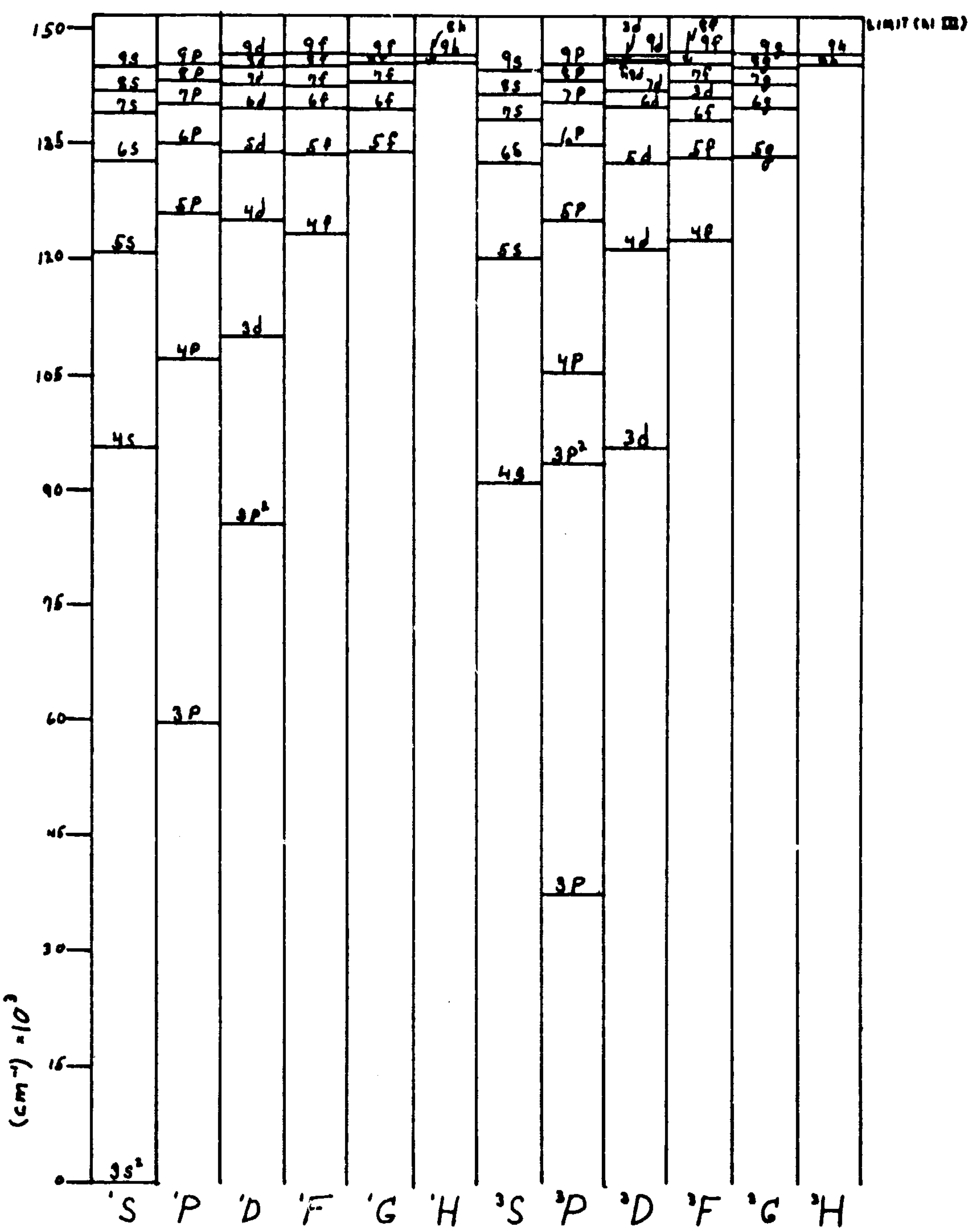

Figure 8. Energy Levels of Al II

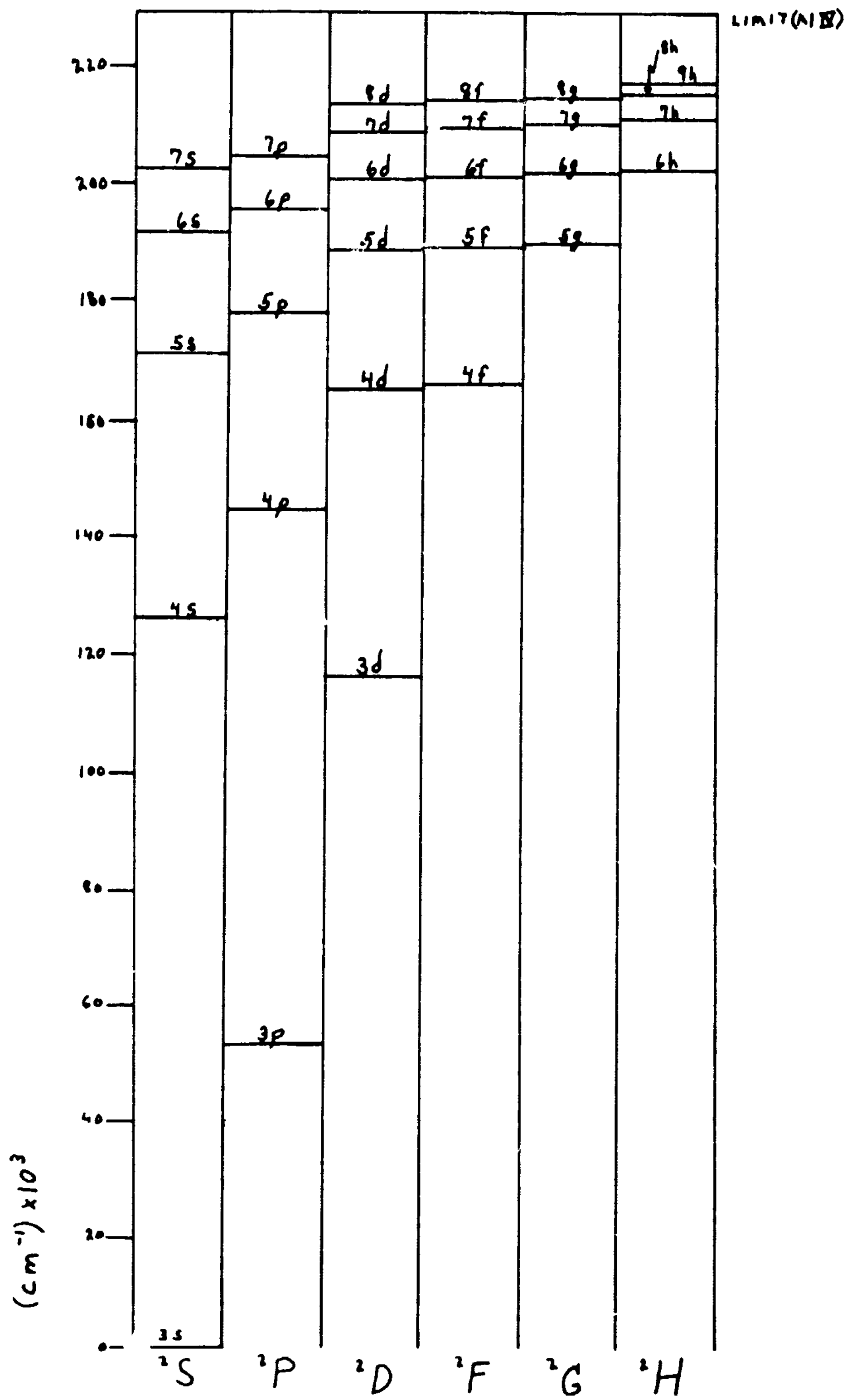

Figure 9. Energy Levels of Al III

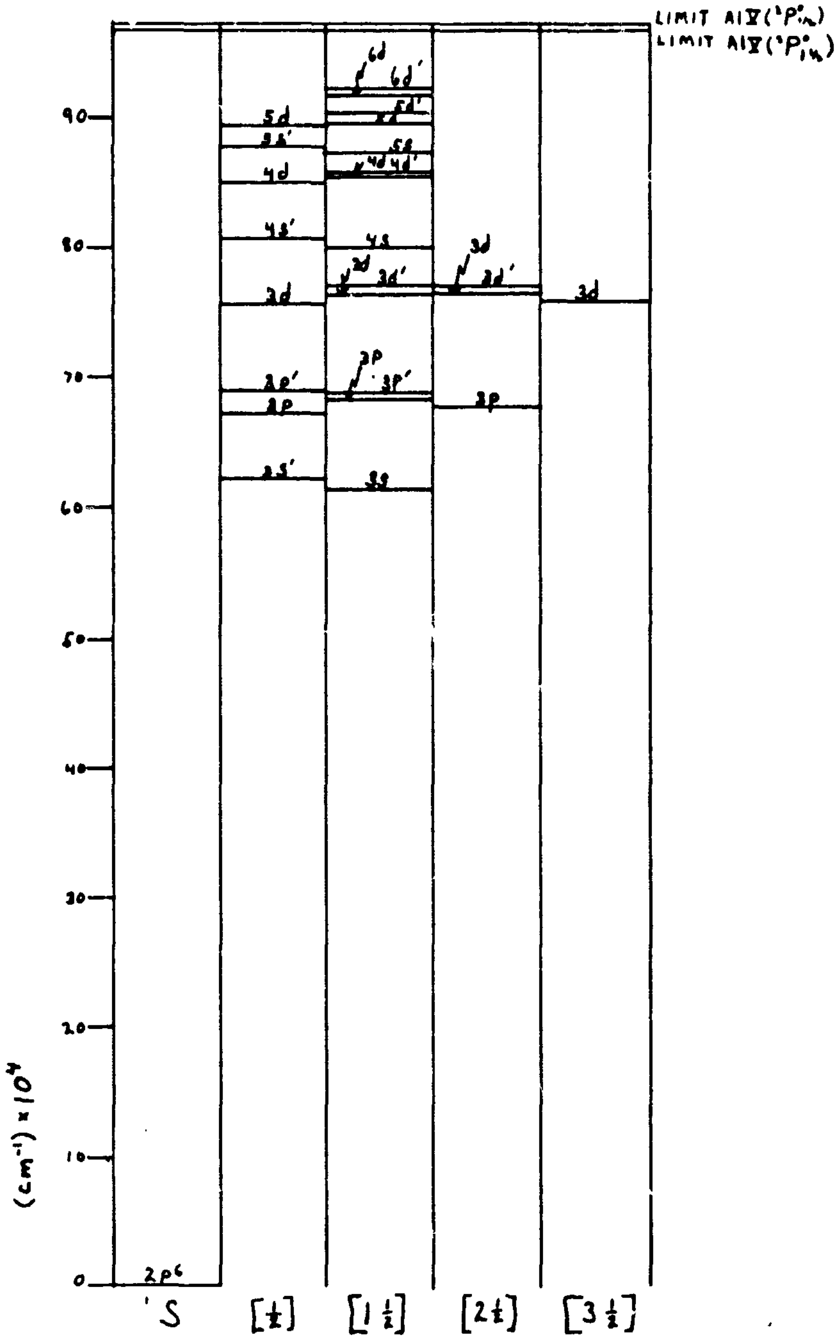

Figure 10. Energy Levels of Al IV

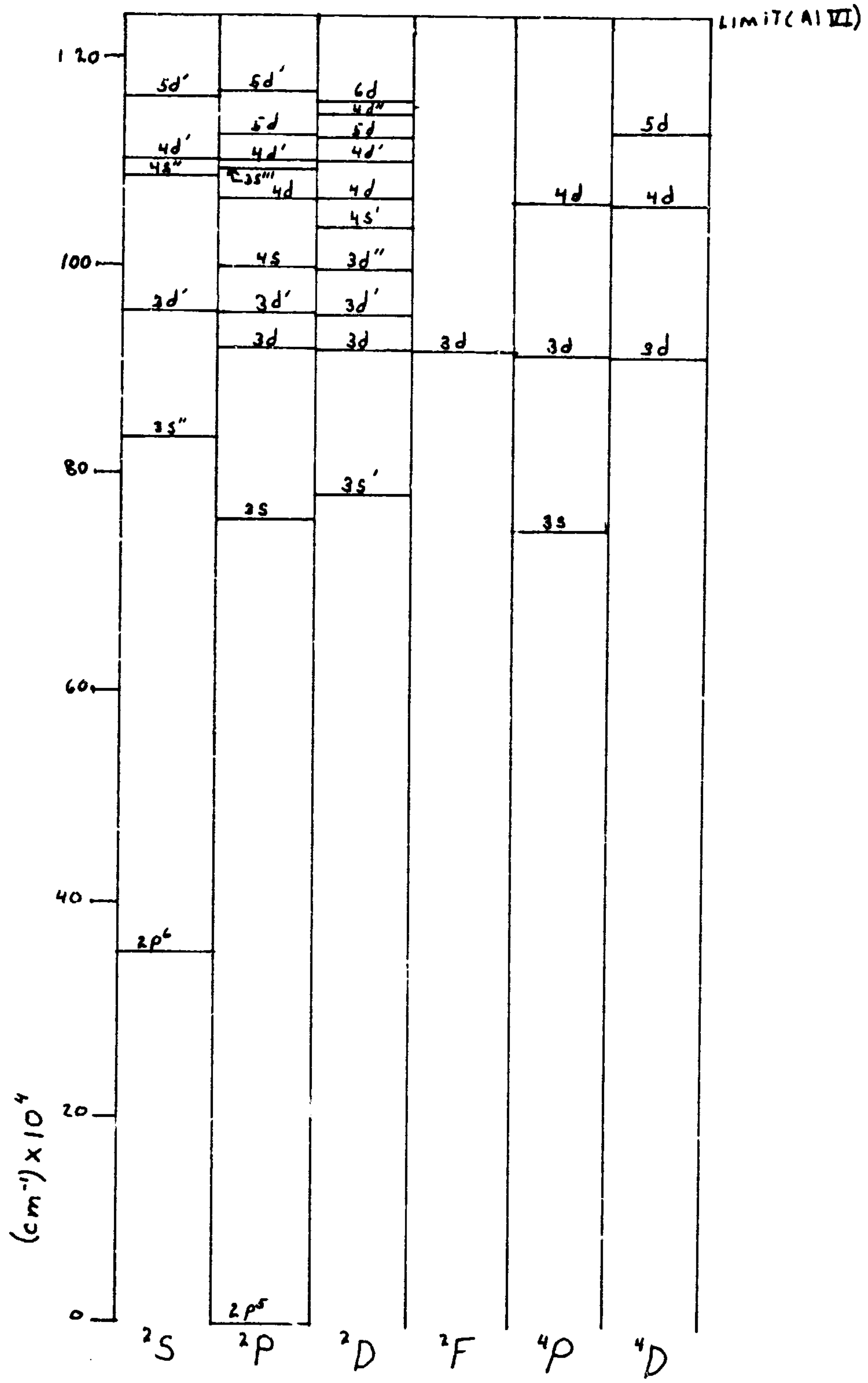

Figure 11. Energy Levels of Al V

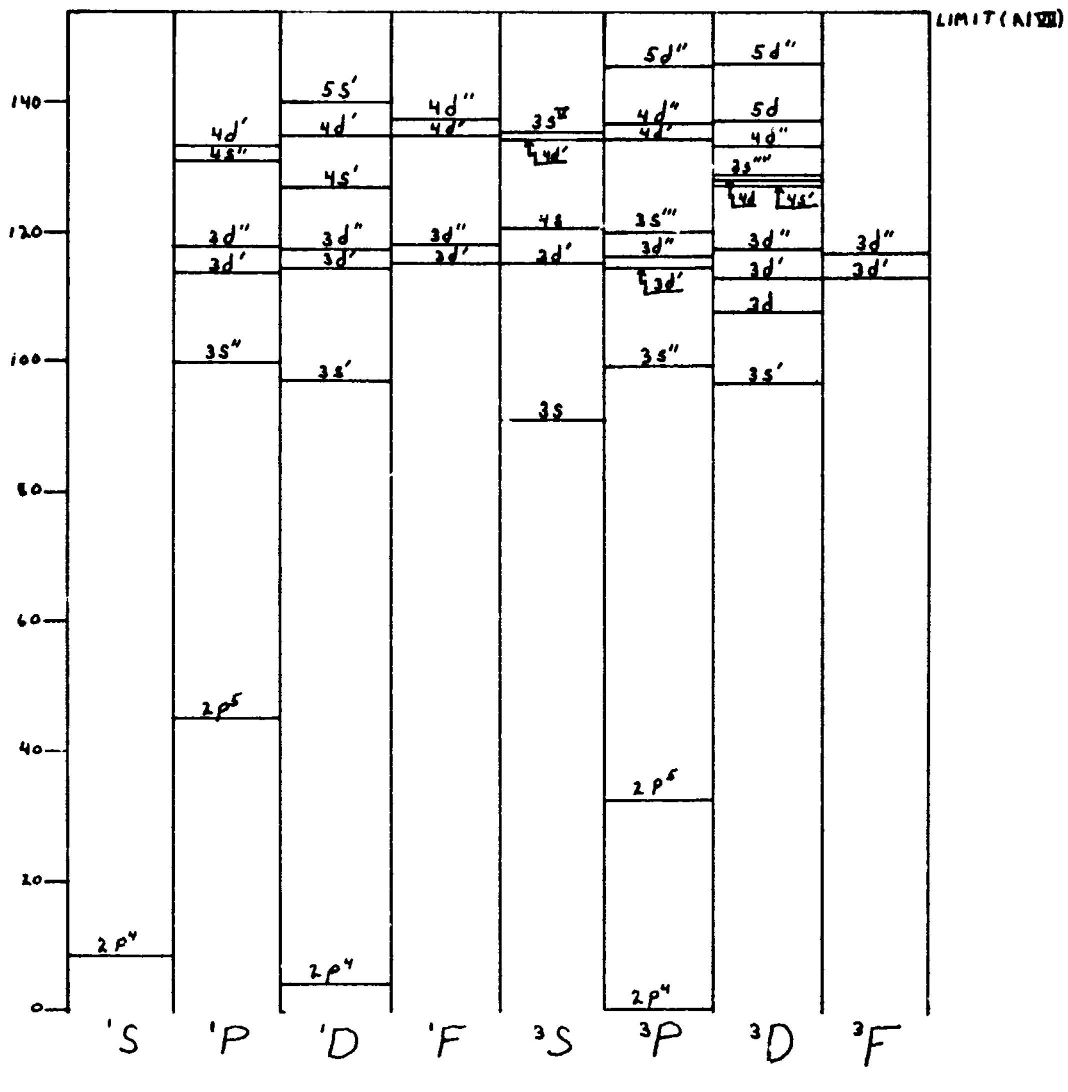

Figure 12. Energy Levels of Al VI

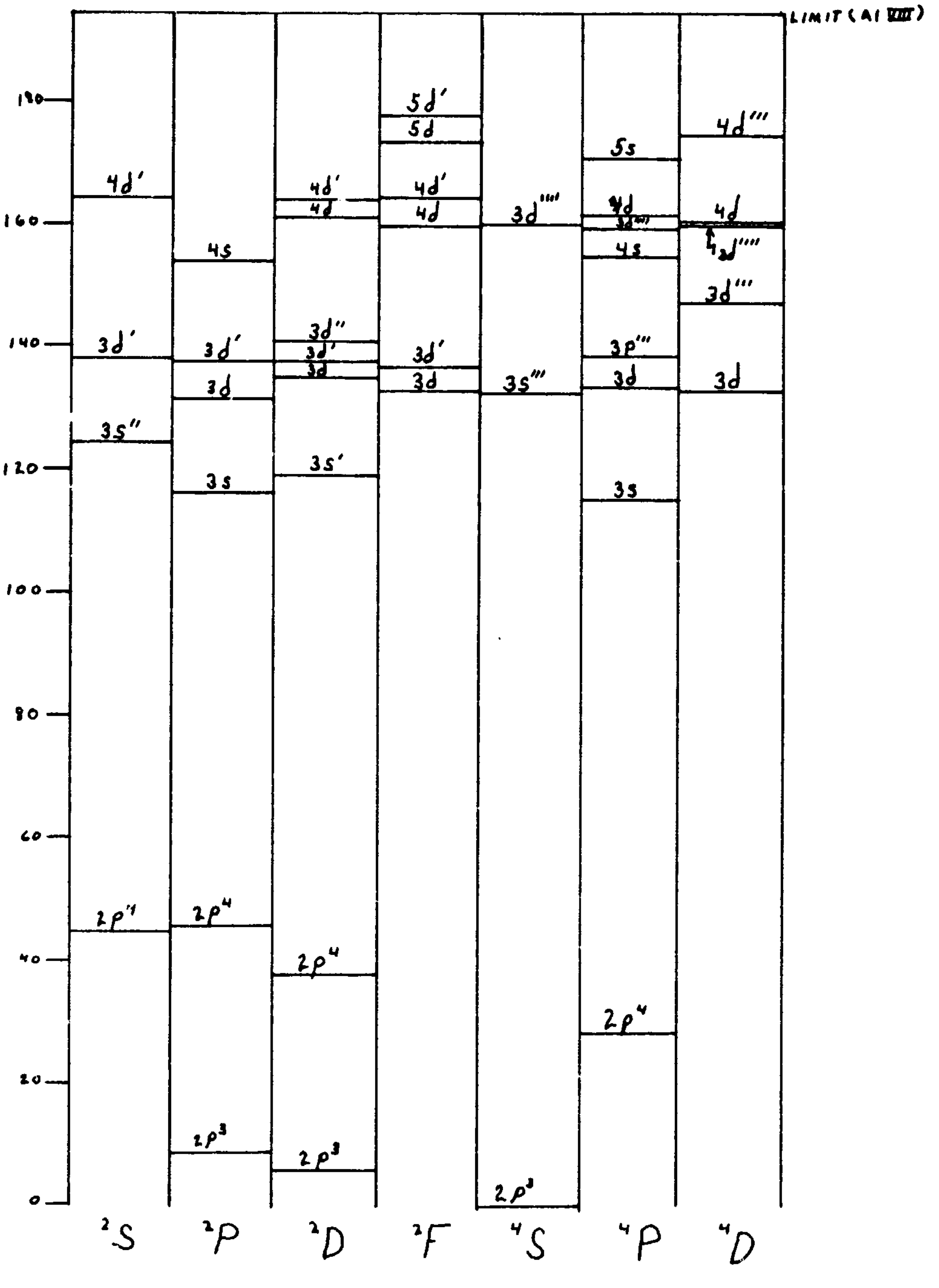

Figure 13. Energy Levels of Al VII

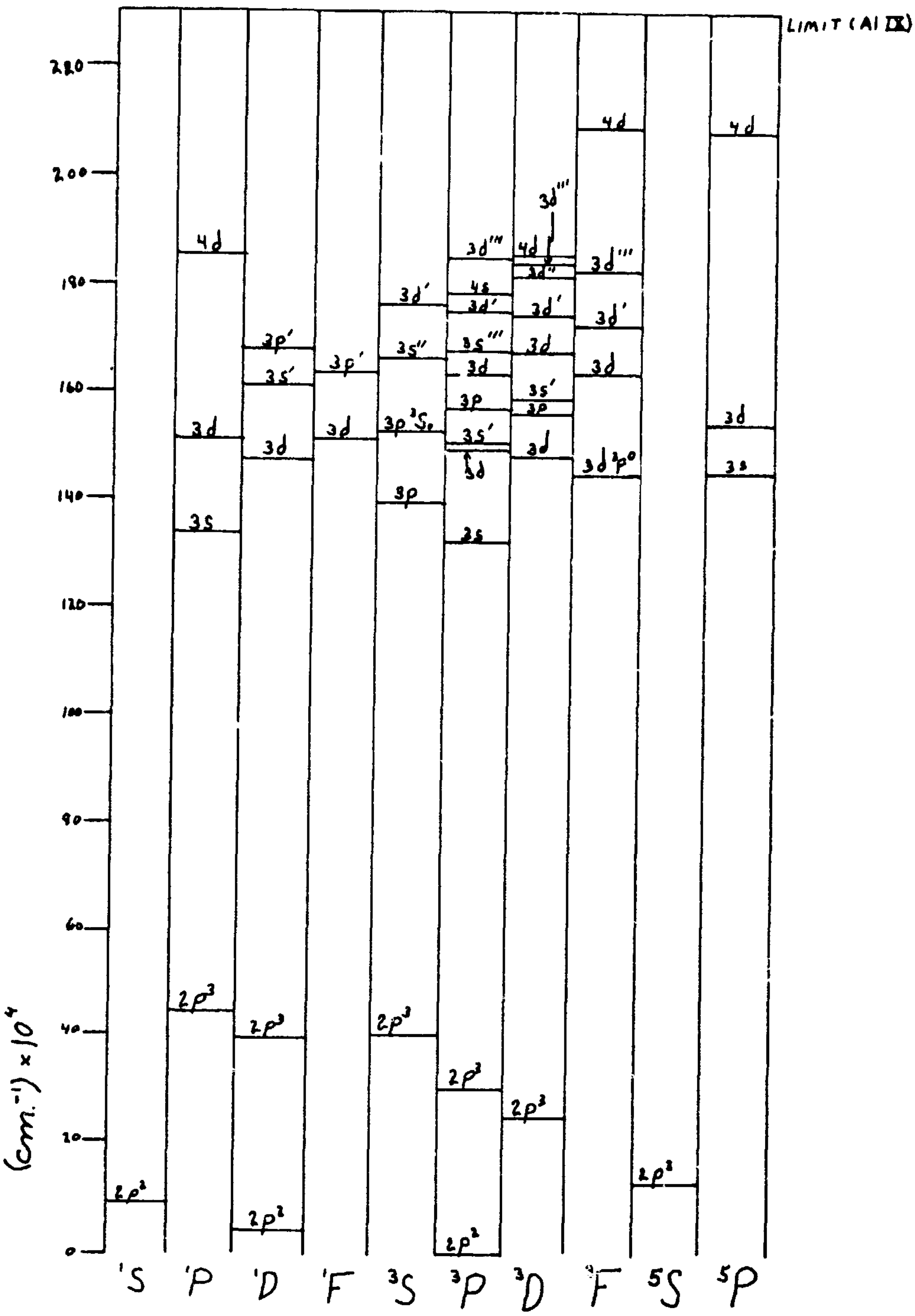

Figure 14. Energy Levels of Al VIII

VITA

Thomas Milton Carpenter

Candidate for the Degree of

Master of Science

Report: CALIBRATION OF A FAR ULTRAVIOLET SPECTROGRAPH AND A STUDY OF VACUUM SPARK BREAKDOWN

Major Field: Physics

Biographical:

Personal Data: Born in Grand Junction, Colorado, February 1, 1943, eldest child of Clyde Elbert and Helen Ethel Carpenter. Married Glenda Jean Wilson on November 26, 1964.

Education: Attended grade school and high school in Grand Junction, Colorado; graduated Valedictorian from Central High School, Grand Junction, Colorado in May, 1961; received Batchelor of Arts degree from Friends University in Wichita, Kansas in May, 1965; completed requirements for Master of Science degree in May, 1970.

Professional Experience: Laboratory Assistant in Department of Chemistry, Friends University, 1963; Honor Assistant in Department of Physics, Friends University, 1964; teaching assistant in Physics Department, Oklahoma State University, 1965; Research Assistant for Research Foundation of Oklahoma State University, 1966-1967; Instructor in Department of Physics, Olivet Nazarene College, 1967-1969; Director of the Computer Laboratory, Olivet Nazarene College, 1968-1969, Member of Sigma Pi Sigma, Oklahoma State University; Member of American Association of Physics Teachers.